EPA-R2-73-235
MAY 1973

Environmental Protection Technology Series

Cation Transport in Soils and Factors Affecting Soil Carbonate Solubility

Office of Research and Monitoring
U.S. Environmental Protection Agency
Washington, D.C. 20460

RESEARCH REPORTING SERIES

Research reports of the Office of Research and Monitoring, Environmental Protection Agency, have been grouped into five series. These five broad categories were established to facilitate further development and application of environmental technology. Elimination of traditional grouping was consciously planned to foster technology transfer and a maximum interface in related fields. The five series are:

1. Environmental Health Effects Research
2. Environmental Protection Technology
3. Ecological Research
4. Environmental Monitoring
5. Socioeconomic Environmental Studies

This report has been assigned to the ENVIRONMENTAL PROTECTION TECHNOLOGY series. This series describes research performed to develop and demonstrate instrumentation, equipment and methodology to repair or prevent environmental degradation from point and non-point sources of pollution. This work provides the new or improved technology required for the control and treatment of pollution sources to meet environmental quality standards.

EPA-R2-73-235
May 1973

CATION TRANSPORT IN SOILS
and
FACTORS AFFECTING SOIL CARBONATE SOLUBILITY

by

Jerome J. Jurinak
Sung-Ho Lai
John J. Hassett

Utah State University
Logan, Utah 84322

Project #13030 FDJ
Program Element #1B2039

Project Officer

Dr. James P. Law, Jr.
U. S. Environmental Protection Agency
Robert S. Kerr Environmental Research Laboratory
P. O. Box 1198
Ada, Oklahoma 74820

Prepared for

OFFICE OF RESEARCH AND MONITORING
U. S. ENVIRONMENTAL PROTECTION AGENCY
WASHINGTON, D. C. 20460

For sale by the Superintendent of Documents, U.S. Government Printing Office, Washington, D.C. 20402
Price $1.25 domestic postpaid or $1 GPO Bookstore

EPA Review Notice

This report has been reviewed by the Environmental Protection Agency and approved for publication. Approval does not signify that the contents necessarily reflect the views and policies of the Environmental Protection Agency, nor does mention of trade names or commercial products constitute endorsement or recommendation for use.

ENVIRONMENTAL PROTECTION AGENCY

ABSTRACT

A predictive model of cation transport in soils was developed and tested. This model involved the definition of the cation exchange process in soil columns during the miscible displacement of cation solutions. A mass balance equation was formulated which included a general nonlinear exchange function. The solution of the equation was accomplished by numerical methods. The method was applied to the transport of cations through an exchanger using five different types of exchange functions. The model was further tested by conducting soil column studies where both homovalent and heterovalent exchange occurred. The agreement between predicted cation transport in soils and experimental data was good.

Laboratory studies were also conducted, using the carbonate saturometer, to assess the effect of Mg^{+2} ion on the solubility of calcareous materials. Carbonate solubility in the presence of Mg^{+2} ion was found to vary with the surface area of the solid phase, the mineralogy of the carbonate material, and the degree of saturation of the water with respect to a given carbonate mineral. Calcite generally increased in solubility, when Mg^{+2} was present, in waters which were unsaturated with respect to calcite. Carbonate material which contained magnesium as a constituent ion, e.g., dolomite, decreased solubility as Mg^{+2} concentration increased in waters which were near saturation with respect to dolomite.

CONTENTS

FIGURES

FIGURES (Continued)

FIGURES (Continued)

TABLES

SECTION I

CONCLUSIONS

A valid predictive model was developed and tested to define the one-dimensional transport of cations in soil columns undergoing miscible displacement by various ionic solutions. The material balance equation used in the model was formulated to incorporate a nonlinear equilibrium exchange function (isotherm equation). This study showed that cation transport through soils was strongly dependent on the equilibrium exchange function which defines a cation's reactivity with the exchange complex of a given soil.

An important parameter in the equilibrium exchange function was the separation factor α_B^A which measures the preference of the soil exchange complex for some cation A over cation B. In terms of water quality, when the value of the separation factor of a soil for a given cation > 1, the cation will be effectively removed from percolating water and irrigation return flow will contain only the cations for which it was exchanged in the soil matrix. The model which was developed not only predicts to what extent a cation will be removed from percolating water in a given soil but when it will eventually make its appearance in the return flow. Correspondingly, when a soil has a separation factor < 1 for a cation in an irrigation water the cation essentially moves with the percolating water and appears immediately in the return flow although its concentration will be reduced from its inflow value. The predictive model estimates the reduced concentration level in the return flow.

This study showed that even when considering cation exchange between similar cations as Mg^{+2} and Ca^{+2} the resulting isotherm is not linear,

i.e., $\alpha_B^A \neq 1$. A general statement is that when considering a total range of possible cation concentrations in soils, the exchange function is nonlinear. However, depending on the portion of the isotherm utilized, the assumption of a linear exchange function may not be in great error.

The predictive model developed for cation transport in soils, under saturated flow conditions, has immediate utility in estimating the quality of irrigation return flow, particularly with reference to soil reclamation. In this case, the model can predict the concentration of both Ca^{+2} and Na^{+} in both the solution and exchanger phase and allows the estimation of how much calcium treated water is required to exchange and displace a given amount of sodium in the soil. In addition, the model can predict the water composition change which can occur during groundwater recharge or the rate of heavy metal accumulation which can occur in a soil when subject to inputs of industrial wastewater. This latter aspect is extremely critical when relating industrial waste disposal to the water quality of receiving streams or groundwater.

The second part of this study was concerned with the effect of Mg^{+2} ion concentration in soil water on the solubility of carbonate material which exists in the matrix. The result in terms of water quality is reflected in an increase or decrease in the total hardness of irrigation return flow. To predict the Mg^{+2} effect on return flow quality requires some knowledge of the soil mineralogy.

When the soil carbonate is pure calcite ($CaCO_3$) and the water is unsaturated with respect to calcite, an increase in the Mg^{+2} ion concentration increases the solubility of calcite. The principle mechanism accounting for this increase in calcite solubility is the

formation if ion-pairs involving the Mg^{+2} ion. Thus, irrigating a soil containing calcite with a water unsaturated relative to calcite and containing Mg^{+2}, would result in an increase in total hardness of the irrigation return flow.

When the solid phase carbonate in a given system contains Mg, e.g. dolomite, as one of its constituents, the presence of Mg^{+2} ion in the water reacts differently than when the carbonate is pure calcite. The data show that, for water far enough removed from saturation with respect to solid phase carbonate, the effect of increasing the concentration of Mg^{+2} in solution will be to increase the amount of carbonate dissolved. However, as the saturation of the water is approached and exceeded, the effect of Mg^{+2} in solution will be to decrease the solubility or increase the precipitation of the carbonate. The initial increase in solubility is ascribed to the formation of ion-pairs involving Mg^{+2}. As the water becomes saturated, the reduction in carbonate solubility is due to the common ion effect of Mg^{+2} which swamps the ion-pair effect. Under field conditions, a soil containing dolomite or a Mg-calcite will enhance the precipitation of carbonate from the percolating water as the Mg^{+2} ion concentration in the water increases. This effect exists if the water is near saturation or supersaturated with respect to the carbonate. Thus, Ca^{+2} and Mg^{+2} will be removed reducing the hardness of the return flow water. If the irrigation water is far removed from saturation, in terms of the soil carbonate material, the presence of Mg^{+2} will increase the solubility of carbonate increasing the hardness of return flow water relative to the irrigation water.

SECTION II

RECOMMENDATIONS

The results of this study show the feasibility of modeling cation transport through soils under saturated flow conditions which allows prediction of the cation composition of irrigation return flow. In principle, the same procedure is adequate to allow predictive modeling of any soluble component that is added to the soil; i.e., herbicides, fertilizers, industrial waste, etc. For example, the modeling of phosphorous or nitrogen movement in soils would produce data valuable to the development of pollution abatement programs.

Since this initial study necessarily involved only controlled laboratory column studies, the full assessment of the model requires expansion into a lysimeter or field study where less control is present and more approximations are required as program inputs. Most normal field conditions involve unsaturated moisture flow; therefore, extension of the model to include unsaturated conditions is a necessary requirement to cover all field situations. Evaluation of multi-cation exchange and soil layering effects must also be included to give the model additional flexibility.

The data from the carbonate solubility study has shown that predicting the effect of irrigation on the total hardness of return flow is not a simple procedure even in refined systems. Chemical data of both the water and soil are required to ascertain whether a given water will dissolve soil carbonate material or whether carbonate will precipitate from a solution. A factor which must be evaluated is the limit of solubility that exists for natural soil carbonates because the data have shown that soil carbonates do not react in the same manner as pure carbonate minerals.

An important aspect of the carbonate precipitation-water quality research should be concerned with the plant growth effect on carbonate precipitation or dissolution from irrigation water. This aspect should involve plant studies in greenhouse or field lysimeters. The objective should be to show the importance of the plant as a sink for water (salt-concentrating agent) and a source of CO_2 in determining how, where, and to what extent carbonate is dissolved or formed from irrigation water. The coupling of chemical water quality data with evapotranspiration and soil CO_2 partial pressure data from the lysimeters will provide valuable information concerning the effect of irrigation of crops on the total hardness of irrigation return flow.

PART A

MODEL FOR
CATION TRANSPORT IN SOILS

SECTION III

INTRODUCTION

Cation adsorption in the soil system is important not only because the soil can be used to modify water quality with respect to the cation composition, but also because it provides a basis for study of water quality treatment with respect to other chemical species which can be adsorbed by soils and other adsorbents.

The cation adsorption operation in resin beds was studied by Hiester and Vermeulen (1952) who used second order kinetics to define the rate of cation exchange. They did not consider the fluid dispersion effect. The same problem was studied by Lapidus and Amundson (1952). They assumed an infinite rate of cation exchange and described the exchange reaction by a linear exchange isotherm. A comparative study of different models of cation adsorption operation was reported by Biggar and Nielsen (1963). Additional studies of the dispersive convective flow through an adsorbent bed were reported by Brenner (1962), Hashimoto et al. (1964) and Lindstrom et al. (1967). Analytical solutions of the material balance equation in the above studies were obtained for certain restricted cases.

In natural soil systems, because of the heterogeneous nature of the pore sequences and slow rate of water flow, the fluid dispersion effect becomes significant and must be considered. In addition, most cation exchange reactions that occur in soil systems do not exhibit linear isotherms. These complications make the analytical solution of the cation adsorption problem formidable.

Biggar et al. (1966) applied the finite plate concept and adopted the computation method developed by Dutt and Tanji (1962) to compare

their numerical computation with the experimental data. The success of the finite plate method depends on the empirical evaluation of the theoretical plate height, which approximates the effects of non-equilibrium condition, fluid dispersion and other disturbances in the column operation. Their study not only included the non-constant separation factor, but also showed the potential of using the numerical method in solving the cation saturation problem in soil columns.

In this study, the finite difference method was applied to the solution of the material balance equation (MBE). The MBE described the dispersive convection flow of the chemical solution and the general adsorption function. The numerical solutions obtained for different adsorption functions show the effect of adsorption on the flow of cations through the adsorbent columns. For linear adsorption, the numerical solution was compared to the analytical solution used by Lindstrom et al. (1967). This comparison provides a measure of the accuracy of the numerical solution. To show the applicability of the numerical solution, column experiments were also conducted involving sodium ion adsorption by Yolo loam soil.

SECTION IV

THEORY AND APPLICATION OF MODEL

The theoretical prediction of one-dimensional cation adsorption in soil columns involved the solution of a material balance equation with given initial and boundary conditions. For the exchange reaction

$$A^+ + BR \leftrightarrows B^+ + AR \qquad [1]$$

where A^+ and B^+ are counter ions (adsorbates), and R is the cation exchanger (adsorbent), the material balance equation for the cation A^+ is

$$D_o \frac{\partial^2 C_A}{\partial z^2} - V_o \frac{\partial C_A}{\partial z} = \frac{\partial C_A}{\partial t} + \frac{\rho}{\epsilon} \frac{\partial q_A}{\partial t} \qquad [2]$$

where C_A is the concentration of the absorbate A in solution, q_A is the amount of the adsorbate A adsorbed per unit weight of the exchanger, z is the depth of the soil column along the direction of the fluid flow, ϵ is the pore fraction, ρ is the bulk density, t is time, V_o is the pore velocity and D_o is the dispersion coefficient. Defining $X_A = C_A/C_o$ and $Y_A = q_A/Q$ where C_o and Q are the total cation concentration in solution and the total cation adsorption capacity, respectively, Equation [2] is reduced to

$$D_o \frac{\partial^2 X_A}{\partial z^2} - V_o \frac{\partial X_A}{\partial z} = \frac{\partial X_A}{\partial t} + \frac{\rho Q}{\epsilon C_o} \frac{\partial Y_A}{\partial t} \qquad [3]$$

The variables X_A and Y_A are the reduced concentration of the solution phase and the adsorbed phase, respectively. They are both functions of z and t.

In this study, it is assumed that equilibrium exists between the cation in solution and the cation adsorbed on the exchanger phase. Thus, at given temperature there is a unique function to relate Y_A to X_A, which is called an adsorption function, or adsorption isotherm. We can express Y_A in terms of X_A

$$Y_A = f(X_A) \qquad [4]$$

and

$$\frac{\partial Y_A}{\partial t} = \frac{dY_A}{dX_A} \frac{\partial X_A}{\partial t} \qquad [5]$$

Substituting Equation [5] into Equation [3] and dropping the subscript, understanding that we are dealing with the adsorbate A^+, we have

$$D(X)\frac{\partial^2 X}{\partial z^2} - V(X)\frac{\partial X}{\partial z} = \frac{\partial X}{\partial t} \qquad [6]$$

where

$$D(X) = \frac{D_o}{1 + \frac{\rho Q}{\epsilon C_o} f'(X)}$$

$$V(X) = \frac{V_o}{1 + \frac{\rho Q}{\epsilon C_o} f'(X)} \qquad [7]$$

and $f'(X) = \frac{dY}{dX}$. Hashimoto et al. (1964) called the term $1 + \frac{\rho Q}{\epsilon C_o} f'(X)$ the retardation factor. The terms D(X) and V(X) are defined as the apparent dispersion coefficient and the apparent pore velocity, respectively. They are functions of X.

The initial and boundary conditions for the cation saturation operation are:

$$\begin{aligned} X(z,0) &= 0 && 0 \leq z \leq L \\ X(0,t) &= 1.0 && t > 0 \\ \frac{\partial X}{\partial z}(L,t) &= 0 && t > 0 \end{aligned} \qquad [8]$$

where L is the length of the column.

The solution of Equations [6] and [8] is obtained by the finite difference method.

Numerical Solution of Model

The partial differential terms in Equation [6] are approximated by the finite differences as follows:

$$\left.\begin{aligned} \frac{\partial^2 X}{\partial z^2} &\simeq \frac{X_{i+1,\,j} - 2X_{i,\,j} + X_{i-1,\,j}}{\Delta z^2} \\ \frac{\partial X}{\partial z} &\simeq \frac{X_{i+1,\,j} - X_{i-1,\,j}}{2\Delta z} \\ \frac{\partial X}{\partial t} &\simeq \frac{X_{i,\,j+1} - X_{i,\,j}}{\Delta t} \\ D(X) &\simeq D(X_{i,\,j}) \\ V(X) &\simeq V(X_{i,\,j}) \end{aligned}\right\} \qquad [9]$$

Δz is the depth increment, Δt is the time increment, i is the subscript for the depth increment and j is the subscript for the time increment.

Substituting Equations [9] into Equation [6] and rearranging the terms we obtain

$$X_{i,j+1} = \Delta t \left(\frac{D(X_{i,j})}{\Delta z^2} - \frac{V(X_{i,j})}{2\Delta z} \right) X_{i+1,j} - \left(\frac{2D(X_{i,j})}{\Delta z^2} - \frac{1}{\Delta t} \right) X_{i,j} + \left(\frac{D(X_{i,j})}{\Delta z^2} + \frac{V(X_{i,j})}{2\Delta z} \right) X_{i-1,j} \quad [10]$$

The initial and the boundary conditions are:

$$\left.\begin{aligned} X_{i,0} &= 0 \\ X_{0,j} &= 1.0 \\ X_{N+1,j} &= X_{N-1,j} \end{aligned}\right\} \quad [11]$$

where i = 1, 2, . . . N; j = 1, 2, . . . M. (N and M are the last number of subscript i and j, respectively.) A FORTRAN program was written to perform the computation of the algorithm in Equations [10] and [11]. The computation was done by a Univac 1108 digital computer. The numerical result obtained approximated the solution X(z, t). The values of Y(z, t) were computed from the values of X(z, t) through the adsorption function, Equation [4].

The numerical solution of this scheme was found to be stable when the grid network spacing was chosen so that

$$0 < \frac{\Delta t}{(\Delta z)^2} < \frac{1}{2}$$

When this was not met, numerical oscillation occurred.

The application of the numerical method for solution of the MBE involving cation adsorption is illustrated by solving example problems. We will take one set of soil column parameters, as shown in Table 1, and solve the equation with five different types of adsorption isotherms and examine the behavior of the concentration functions of the solution phase X(z, t) and that of the adsorbed phase Y(z, t), obtained from the solution in form of cation concentration profiles.

Table 1. The Column Parameters

ITEM	UNIT	VALUE
Pore velocity, $\bar{V}$	cm/hr	1.50
Dispersion coefficient, D	cm^2/hr	1.50
Bulk density, ρ	g/cm^3	1.30
Pore fraction, ϵ		0.45
Cation adsorption capacity, Q	meq/g	0.25
Total cation concentration, C_o	meq/cm^3	0.10
Column length, L	cm	30.00
Pore volume	ml	612.50
Depth increment used	cm	0.50
Time increment used	hr	0.10

The behavior of the adsorption functions depend mainly on (1) the type of adsorbent, (2) the adsorbate involved, and (3) the total concentration of the adsorbate. The five adsorption functions selected for this study are shown in Figure 1. They can be represented by a general equation:

$$Y = \frac{X}{X + (1-X)/\alpha_B^A (X)} \qquad [12]$$

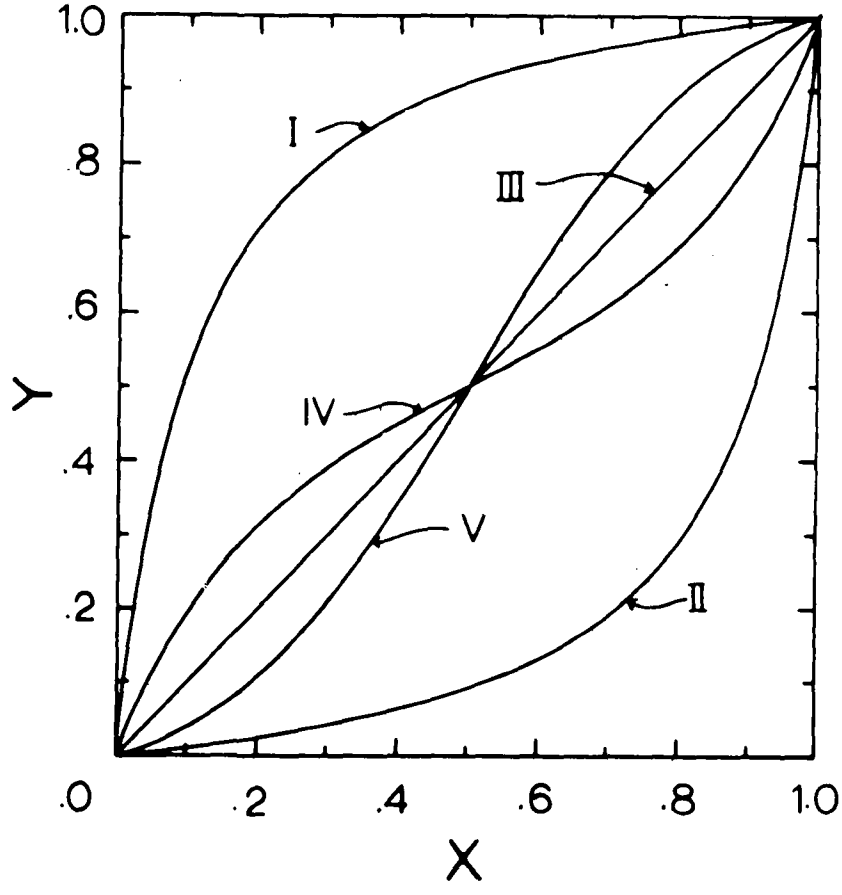

Figure 1. The five representative types of isotherms used in the study.

where $\alpha_B^A(X)$ is a function called the separation factor defined by Helfferich (1962) as $\alpha_B^A = \frac{Y_A X_B}{Y_B X_A}$. It described the relative distribution of the adsorbates between the adsorbent and the solvent. The separation factor is either a constant or a function of the composition X. For the exchange functions of Type I, II and III, as shown in Figure 1, the separation factors are constant and have a value equal to 10, 0.1 and 1.0, respectively. For the exchange functions of Type IV and V, $\alpha_B^A(X)$ is a function of X and can be represented as

$$\alpha_B^A(X) = \frac{1}{\exp[\ln K + c(1-2X)]} \qquad [13]$$

where K is the thermodynamic equilibrium constant and c is a proportionality constant which accounts for adsorbate interaction. This adsorption function is referred to as the Kielland function (Helfferich, 1962). The value of K for Type IV and Type V adsorption functions is arbitrarily set equal to 1.0 and the value of c is -1.0 and +1.2, respectively.

The solution of the MBE, in terms of X(z,t) and Y(z,t) for each adsorption function, is presented in Figures 2 through 6 as concentration profiles with time as a parameter.

Isotherm Shape

The isotherms or part of the isotherm in Figure 1 can be classified according to the value of the separation factor:

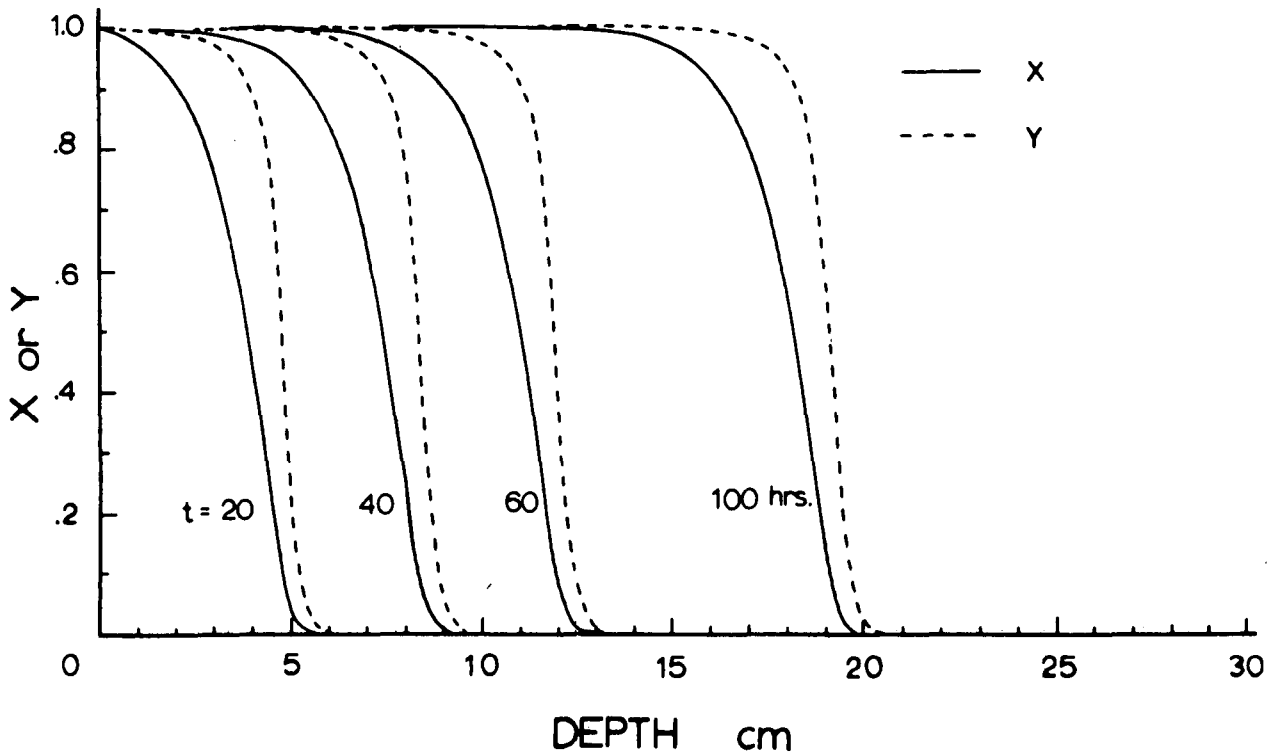

Figure 2. The cation concentration profiles X(z, t) and Y(z, t) computed from the Type I isotherm.

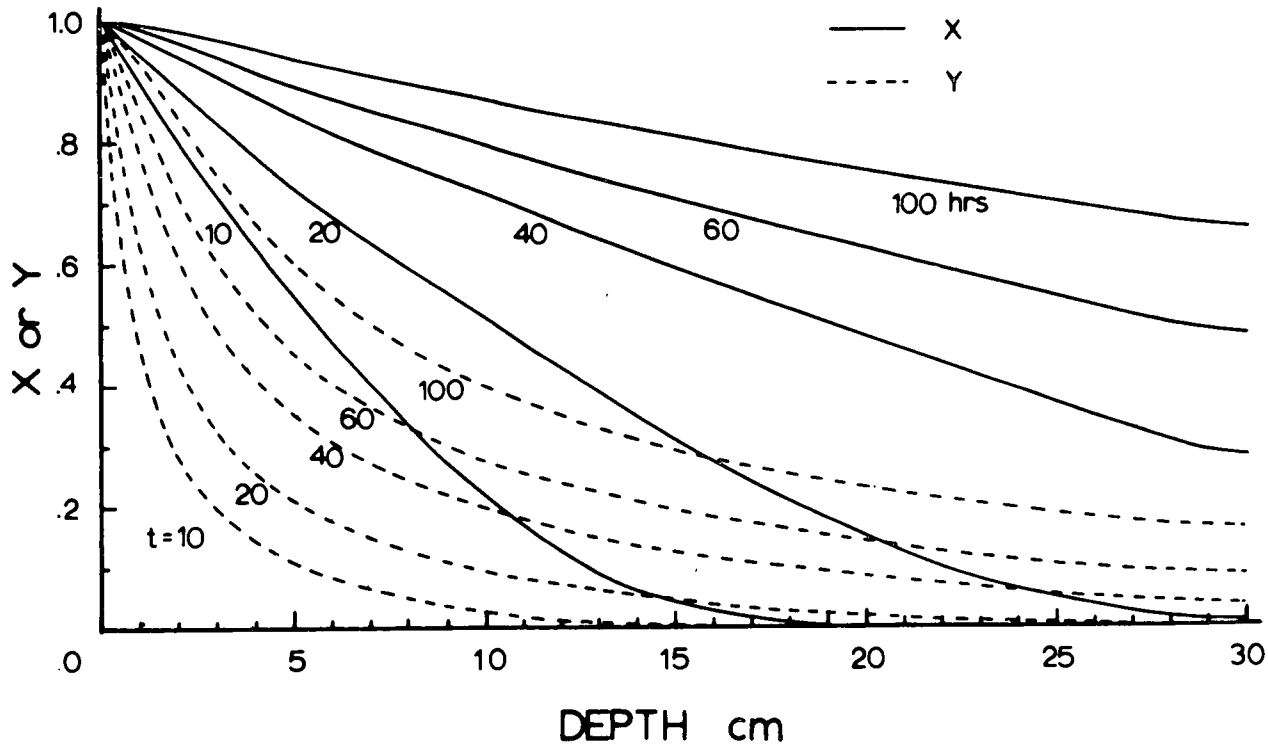

Figure 3. The cation concentration profiles X(z, t) and Y(z, t) computed from the Type II isotherm.

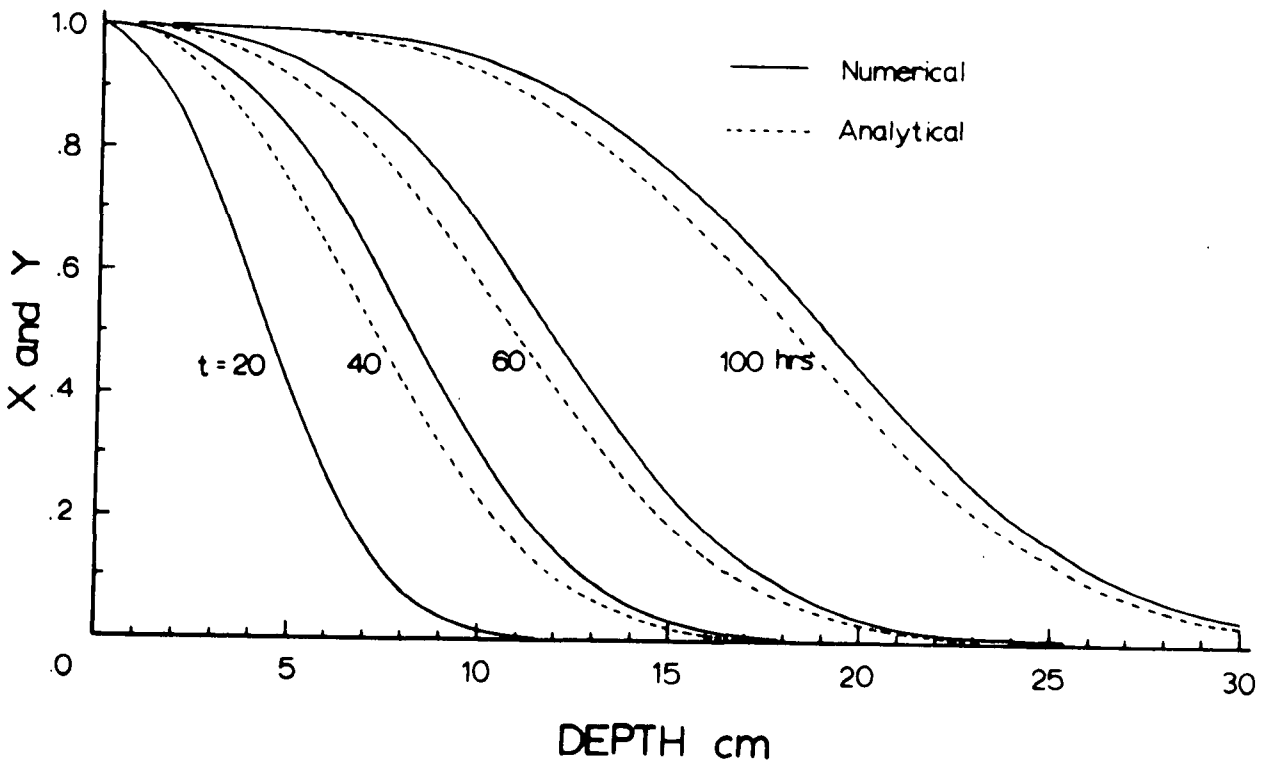

Figure 4. The cation concentration profiles X(z, t) and Y(z, t) computed from the Type III isotherm by numerical and analytical methods.

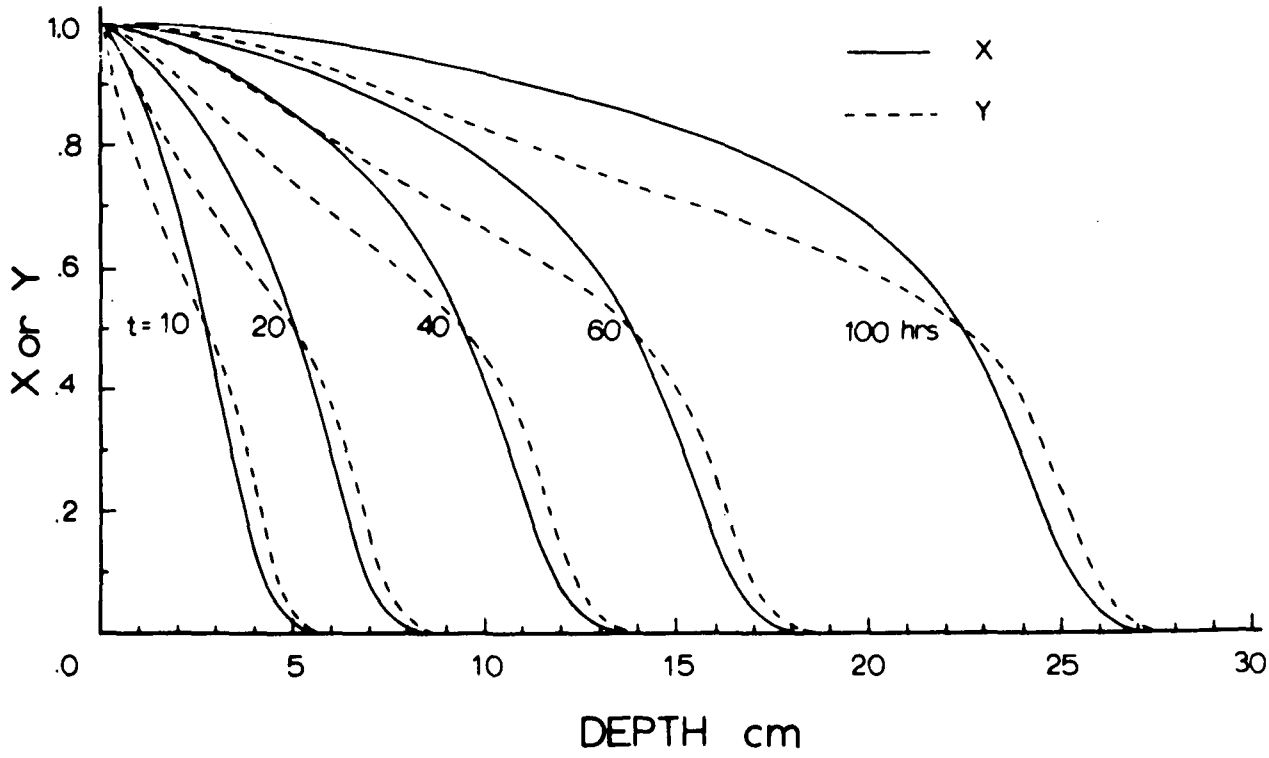

Figure 5. The cation concentration profiles X(z, t) and Y(z, t) computed from the Type IV isotherm.

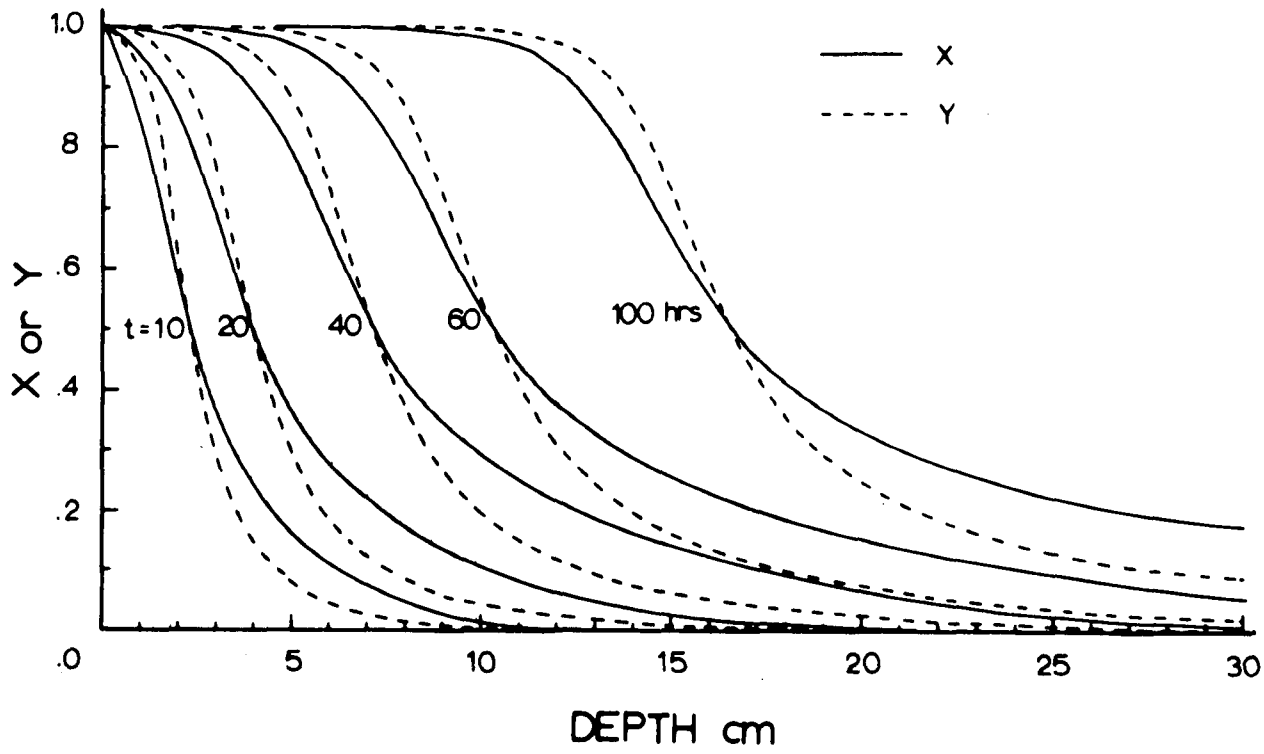

Figure 6. The cation concentration profiles X(z, t) and Y(z, t) computed from the Type V isotherm.

(1)	Convex isotherm	$\alpha_B^A > 1$
	Type I	$0. < X < 1.0$
	Type IV	$0. < X < 0.5$
	Type V	$0.5 < X < 1.0$
(2)	Concave isotherm	$\alpha_B^A < 1$
	Type II	$0. < X < 1.0$
	Type IV	$0.5 < X < 1.0$
	Type V	$0. < X < 0.5$
(3)	Linear isotherm	$\alpha_B^A = 1$
	Type III	$0. < X < 1.0$

Convex Isotherm. The fixed-bed adsorption of cations that exhibit convex isotherms is characterized by (1) sharp concentration profiles, (2) an approximately steady state advancement of the profiles, and (3) the adsorbed phase profiles preceding the solution phase profiles. These properties are shown in Figure 2; in Figure 5, when $0 < X, Y < 0.5$; and in Figure 6, when $0.5 < X, Y < 1.0$.

Two factors affecting dispersion are (1) the nature of the pore sequences in the matrix (physical dispersion) and (2) the shape of the adsorption isotherm. For a convex isotherm $f'(X)$ is a decreasing function of X while V and D are increasing functions of X, thus, dispersion is suppressed. When the two factors balance each other, the advancing profiles reach a steady state and assume parallel positions as shown in Figure 2.

The separation factor for convex isotherms is greater than unity ($\alpha_B^A > 1.0$) which favors cation adsorption. Thus, the profile of the

adsorbed phase advances ahead of the solution phase profile. This operation is efficient in the removal of the adsorbate from the solvent.

Concave Isotherm. Fixed-bed cation adsorption described by a concave isotherm is characterized by (1) increasingly diffused concentration profiles, and (2) the lagging of the adsorbed phase profile behind the solution phase profile. These features are shown in Figure 3; in Figure 5 when $0.5 < X,\ Y < 1.0$; and in Figure 6 when $0 < X,\ Y < 0.5$.

The $f'(X)$ of a concave isotherm is an increasing function of X, and V and D are decreasing functions of X. The result is an increase in the spreading of the adsorbate along the direction of flow in addition to physical dispersion. Rachinskii (1965) concluded that the dispersion of the profiles due to the concavity of the isotherm is proportional to t, while that due to physical dispersion is proportional to $t^{1/2}$. The concavity of the isotherm is an important cause of dispersion as seen by comparing Figure 3 with Figure 4. The latter figure only involves physical dispersion. Since $\alpha_B^A < 1$, the adsorption of the cation from solution is not favored. Hence, the solution phase profile precedes the adsorbed phase profile. The adsorption of Na^+ in the Ca-soil system is an example of this case. Experimental data are presented later (Section VI).

Linear Isotherm. The linear isotherm is intermediate between the convex and concave isotherms. Figure 4 shows the concentration profiles for the linear isotherm case. Profile characteristics are: (1) the dispersion of the profiles increase with time, and (2) the adsorbed phase and solution phase profiles are identical.

The values of D and V are constant in a linear isotherm system, hence, the solution of the MBE is the same as that involving nonadsorbed

chemical species. However, the profile advancement, compared to that of a nonadsorbed species is reduced by the retardation factor. Because $\alpha_B^A = 1$, there is an equal distribution of the adsorbate between phases.

Verification of the Numerical Solution

The numerical solution of the MBE was checked for accuracy, in the linear isotherm case, by comparison with the analytical solution. The analytical solution used was reported by Lindstrom et al. (1967) as:

$$C/C_o = 1/2 \left[\operatorname{erfc}\left(\frac{z-Vt}{(4Dt)^{1/2}}\right) + \left(\frac{4V^2t}{D\pi}\right)^{1/2} \exp - \left(\frac{z-Vt}{(4Dt)^{1/2}}\right)^2 - \frac{V}{D}\left(\frac{D}{V} + Vt + z\right) \exp\left(\frac{zV}{D}\right) \operatorname{erfc}\left(\frac{z+Vt}{(4Dt)^{1/2}}\right)\right] \quad [14]$$

The analytical and numerical solutions are shown in Figure 4. The discrepancy between the two solutions of the MBE was less than 10 percent for all profiles. The accuracy of the numerical solution for the other isotherm types should be comparable to that of the linear case, although the concave isotherm may be more prone to numerical error.

The error related to the numerical solution of the MBE is referred to as "numerical dispersion" (Bredehoeft, 1971; Oster et al., 1970; Pinder and Copper, 1970). This error is largest when the pore velocity is high. The discrepancy between the numerical and analytical solution shown in Figure 4 is independent of time. The error is well confined and is believed to originate during the early stages of computation when the boundary singularity exists. During diffusive, convective flow involving adsorption, the apparent pore velocity and apparent dispersion

coefficient are both reduced by the retardation factor. This makes the numerical scheme less vulnerable to numerical dispersion (Oster, 1971).

SECTION V

MATERIALS AND METHODS

The columns used in this study consisted of eleven lucite rings, with an inside diameter of 7.6 cm, separated by rubber gaskets and joined together with three threaded brass bars. The effluent end of the column contained a porous plate inbedded in a lucite plate with an outlet at the center.

The column was packed uniformly with soil to a depth of about 24 cm. It was initially saturated with a 0.1 N $CaCl_2$ solution until it reached steady state with respect to the Ca^{++} ion. The miscible displacement was conducted by adding 0.1 N $MgCl_2$ or 0.1 N NaCl exchanging solution. When a predetermined amount of the exchanging cation solution had been added to the column, the flow was terminated and the column sectioned into eleven portions. The soil solution in each section was extracted and the soil air dried. The cations in the extracts, and the exchangeable cations of the soil were determined for each section.

The average interstitial flow velocity was used since only a slight change of the flow rate was detected throughout the experiment. The fluid dispersion coefficient was determined for each column before the miscible displacement experiment by obtaining the chloride breakthrough curve and applying the equation of Rifai et al. (1956) to calculate the $D/\overline{V}$ ratio

$$D/\overline{V} = \frac{L}{4\pi V_o^2 S_o^2} \qquad [15]$$

where L is the length of the column, V_o is the effluent volume at the chloride concentration $C/C_o = 0.5$, which is also the apparent pore volume used in the study, and S_o is the slope of the breakthrough curve at $C/C_o = 0.5$. The column parameters for the experiments are presented in Tables 2 and 3.

The exchange isotherm was obtained by plotting the normalized concentration in the solution X against the normalized concentration in the adsorbed phase Y obtained from each section of the column. The exchange function was then obtained by fitting the experimental value of X and Y into the Equations [12] and [13].

The soils used in this study were Yolo loam and Hanford sandy loam from California and Nibley clay loam from Utah. Three column experiments, using different total volumes of miscible displacing solution, were conducted with each soil.

Table 2. The Column and Soil Parameters for Miscible Displacement Studies Involving Magnesium Adsorption

Items	Unit	Yolo Loam Column			Nibley Clay Loam Column			Hanford Sandy Loam Column		
		I	II	III	I	II	III	I	II	III
Flow velocity, $\overline{V}$	cm/hr	3.936	4.712	3.688	1.043	1.227	1.974	1.284	1.302	1.452
Dispersion coefficient, D	cm^2/hr	1.875	2.245	1.757	1.268	1.492	1.471	0.316	0.327	0.481
Bulk density, ρ	g/cm^3	1.284	1.295	1.303	1.332	1.332	1.307	1.602	1.604	1.591
Pore fraction, ϵ		0.406	0.406	0.441	0.446	0.446	0.467	0.358	0.351	0.378
Cation exchange capacity, Q	me/g	0.257	0.262	0.274	0.266	0.285	0.308	0.057	0.059	0.068
Total concentration, C_o	me/ml	0.105	0.104	0.105	0.107	0.111	0.111	0.108	0.108	0.107
Column length, L	cm	24.7	24.7	23.6	23.5	23.5	23.6	24.0	24.5	22.6
Total time, t	hr	14	25	40	20	50	50	15	30	43
Pore volume, V_o	ml	455	455	472	475	475	500	390	390	388
Total input volume	ml	1015	2170	2950	430	1240	2090	313	622	1072
Total input volume	(pore volume)	2.231	4.770	6.248	0.905	2.611	4.180	0.803	1.595	2.763

Table 3. The Basic Column and Soil Parameters for Miscible Displacement Studies Involving Sodium Adsorption

Items	Soil: Yolo Loam Unit	Column 1	Column 2	Column 3
Pore velocity, $\overline{V}$	cm/hr	7.373	3.732	5.343
Dispersion coefficient, D	cm^2/hr	0.950	0.286	0.797
Bulk density, ρ	g/cm^3	1.306	1.312	1.302
Pore fraction, ϵ		0.470	0.491	0.460
Cation adsorption capacity, Q	meq/g	0.248	0.250	0.241
Total concentration, C_o	meq/ml	0.106	0.105	0.105
Column length, L	cm	23.0	23.1	23.0
Total time, t	hr	4.0	10.0	10.0
Pore volume	ml	490.0	515.0	480.0
Total input volume	ml	628.3	832.0	1121.4
Total input volume	(pore volume)	1.282	1.616	2.336

SECTION VI

RESULTS AND DISCUSSION

Comparison of the Linear and the Nonlinear Models

The model of Lapidus and Amundson, which expressed the cation exchange isotherm as a linear function, i.e., $Y = a + bx$, is compared to the nonlinear model in which the cation exchange function is expressed by the nonlinear modified Kielland function, Equation [13]. The predictions obtained from the two methods were compared to the experimental data obtained from the soil columns.

The cation exchange isotherm of the Mg → Ca exchange for Yolo loam soil is presented in Figure 7. The broken line represents the linear regression line of the experimental data in the form of $Y = a + bx$ with the value of a and b equal to .04 and .92, respectively. The solid line represents the modified Kielland function expressed in Equations [12] and [13] with lnK and c equal to .0855 and -.475, respectively. The results of the numerical computation for the value of $X(z, t)$ obtained from these two methods are presented as concentration profiles in Figure 8, along with the experimental results. The values of $Y(z, t)$ were obtained from the exchange functions using the computed values of $X(z, t)$. These results are presented in Figure 9, together with the experimental results.

Figure 8 shows that the values computed from the nonlinear exchange function agree with the experimental data better than those computed from the linear function. This is particularly true in the higher concentration region where $0.4 \leq X \leq 1.0$. The exchange isotherm, in Figure 7, also shows that the nonlinear form of the isotherm represents

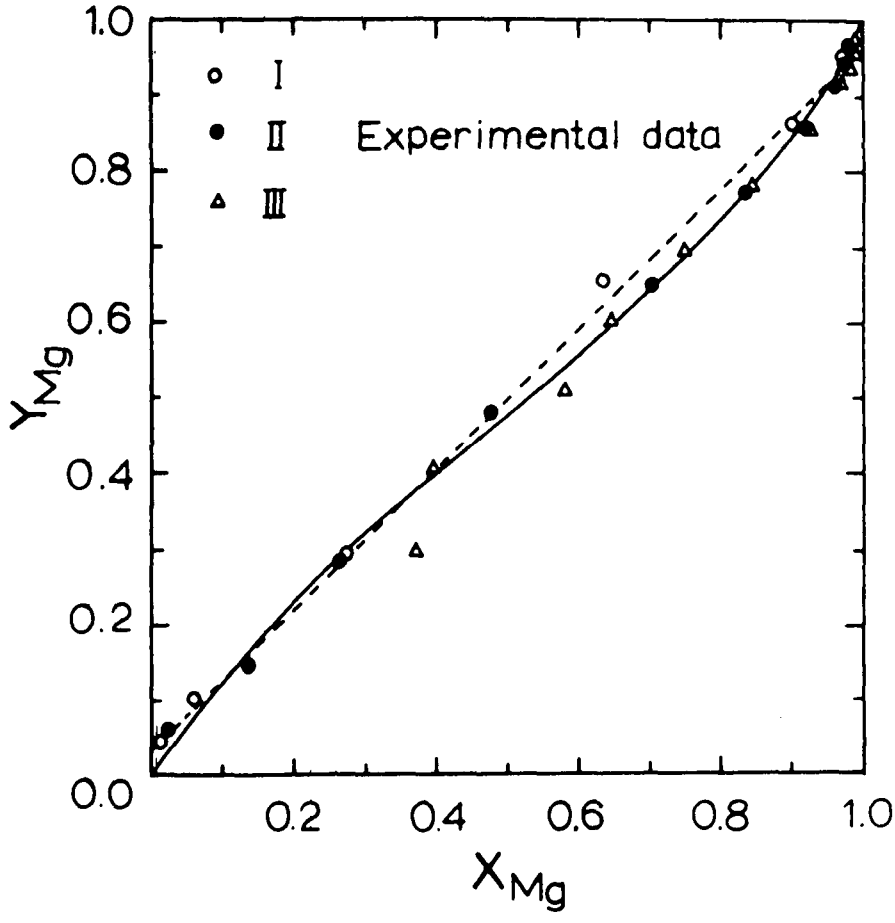

Figure 7. The normalized cation exchange isotherm of the Mg → Ca exchange for Yolo loam soil. The broken line is the linear regression line. The solid line is the modified Kielland function.

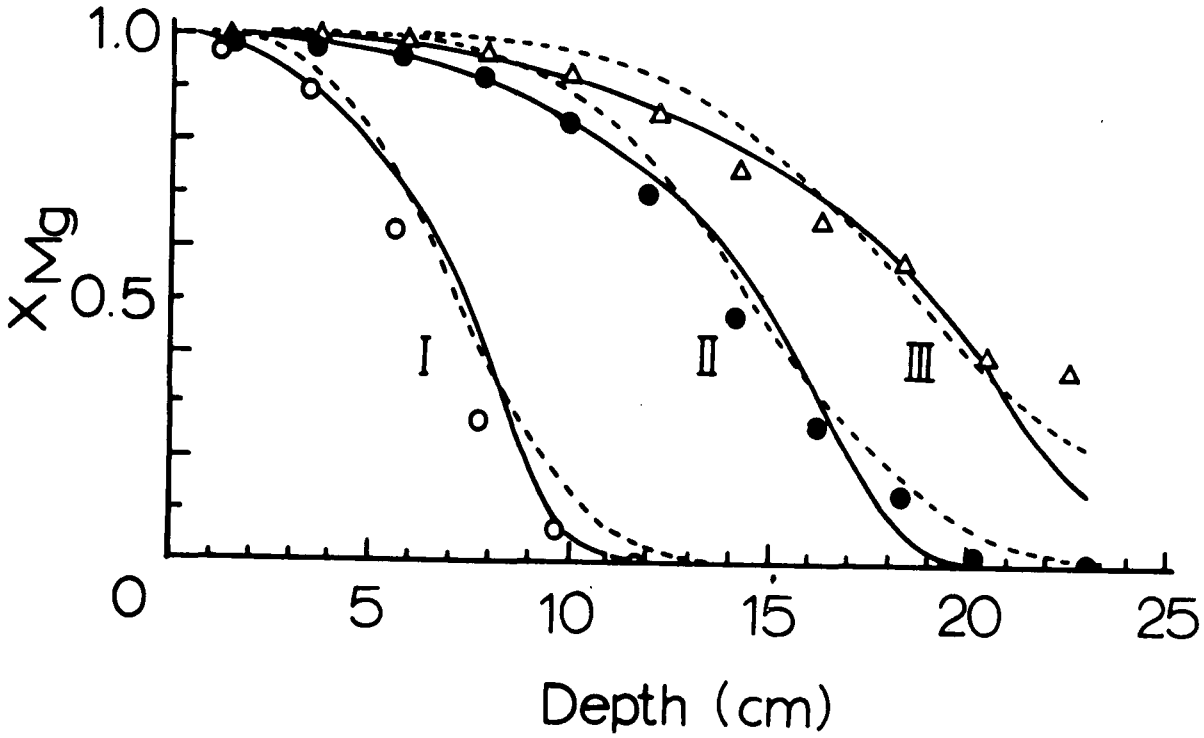

Figure 8. The normalized concentration profiles of the solution phase for the three Yolo loam columns, including both experimental and theoretical values calculated from the linear exchange function (broken lines), and from the modified Kielland function (solid lines).

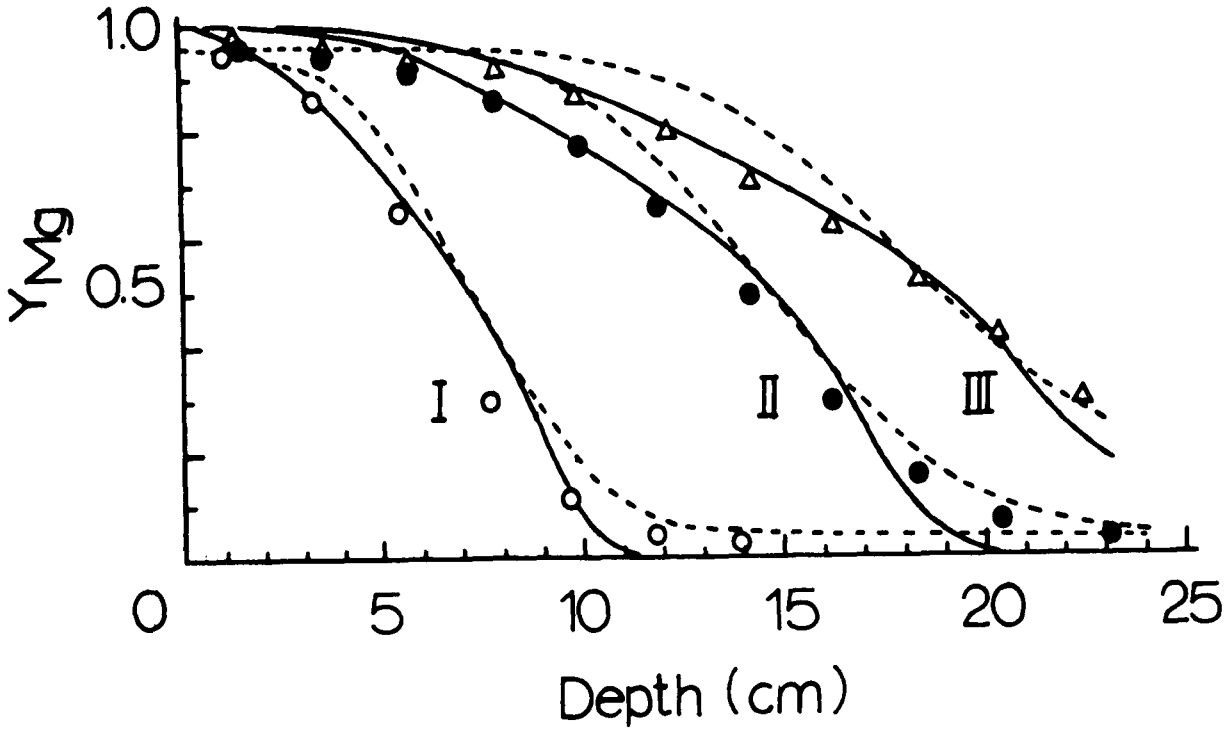

Figure 9. The normalized concentration profiles of the adsorbed phase for three Yolo loam columns, including both experimental and theoretical values calculated from the linear exchange function (broken lines), and from the modified Kielland function (solid lines).

the experimental values more closely than the linear form. The nonlinear fit is superior not only in the actual position of the isotherm but also in the shape of the isotherm. It is emphasized that in the theoretical computation, the slope of the isotherm f' (X) is involved in the evaluation of $g(X_{i,j})$, see Section IV, thus both the position and the shape of the isotherm are important in obtaining the theoretical solution. Biggar and Nielsen (1963) concluded that one of the reasons for the disagreement of the Lapidus and Amundson model with experimental data could be due to an inadequate description of the exchange function. This study gives evidence to support their conclusion. The cation exchange theory dictates that the isotherm must pass through the two points having the X and Y coordinates of (0, 0) and (1, 1). Only one straight line exists between these two points, thus the linear isotherm is the line Y = X.

The linear isotherm may be expected in the situation where the soil exhibits no preference for either of the cations involved in exchange, e. g., isotopic cation exchange. Another case may be when only a trace of cation is introduced into the column and only a small portion of the isotherm is involved in the computations, and a linear approximation of this portion of the isotherm may be adequate. It is expected, however, that nonlinear isotherms are normal in soil systems.

Results shown in Figure 9 also indicate that the Y(z, t) profiles computed with the nonlinear function agree with the experimental value better than the ones calculated with the linear function. From the linear exchange function the calculated value of Y varies between 0.04 and .96 when X varies between 0.0 and 1.0. Thus, according to the linear isotherm, the column can never be saturated with either Mg^{++} or Ca^{++} This is theoretically unsound.

Application of the Nonlinear Model to Mg → Ca Exchange

The nonlinear method was also applied to the Mg → Ca exchange for Nibley clay loam and Hanford sandy loam. The Mg → Ca cation exchange isotherms for the Nibley clay loam and the Hanford sandy loam are presented in Figures 10 and 11, respectively. The experimental data were fitted into the modified Kielland function with the values of lnK and c equal to .4048 and -.92, respectively, for the Nibley clay and equal to .377 and -.725, respectively, for the Hanford sandy loam. The normalized concentration profiles for the solution phase X(z, t) and for the adsorbed phase Y(z, t) are presented in Figures 12 and 13, respectively, for the Nibley clay loam. The same data, for Hanford sandy loam, are presented in Figures 14 and 15.

Figures 12 and 15 show that the agreement between the experimental results and the theoretical computation is good both in the position and shape of the profiles. However, a slight discrepancy was noted between the experimental values and the computed values at the advancing front of the profiles. This difference tended to increase with time. Discussion of these data will be presented later.

Figure 11 shows that the Mg → Ca exchange isotherm for Hanford sandy loam at a total concentration of 0.1 N is nonlinear. The separation factor, α_B^A, is a function of the ionic composition. The modified Kielland function closely represents the isotherm, except in the higher concentration range.

Figure 14 shows that the agreement between the experimental and the theoretical profiles is reasonable for the first two columns. For the third column, the agreement is fair with respect to both the actual position and the shape of the profiles. Similar observation can be

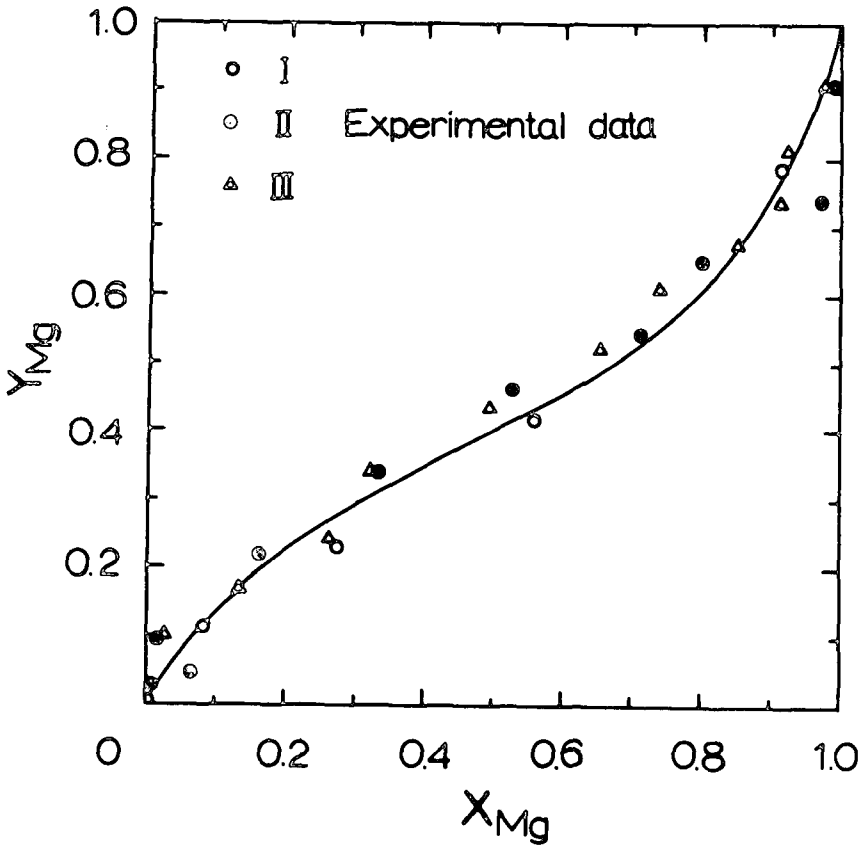

Figure 10. The normalized cation exchange isotherm of the Mg → Ca exchange for Nibley clay loam soil with the modified Kielland function shown by the solid line.

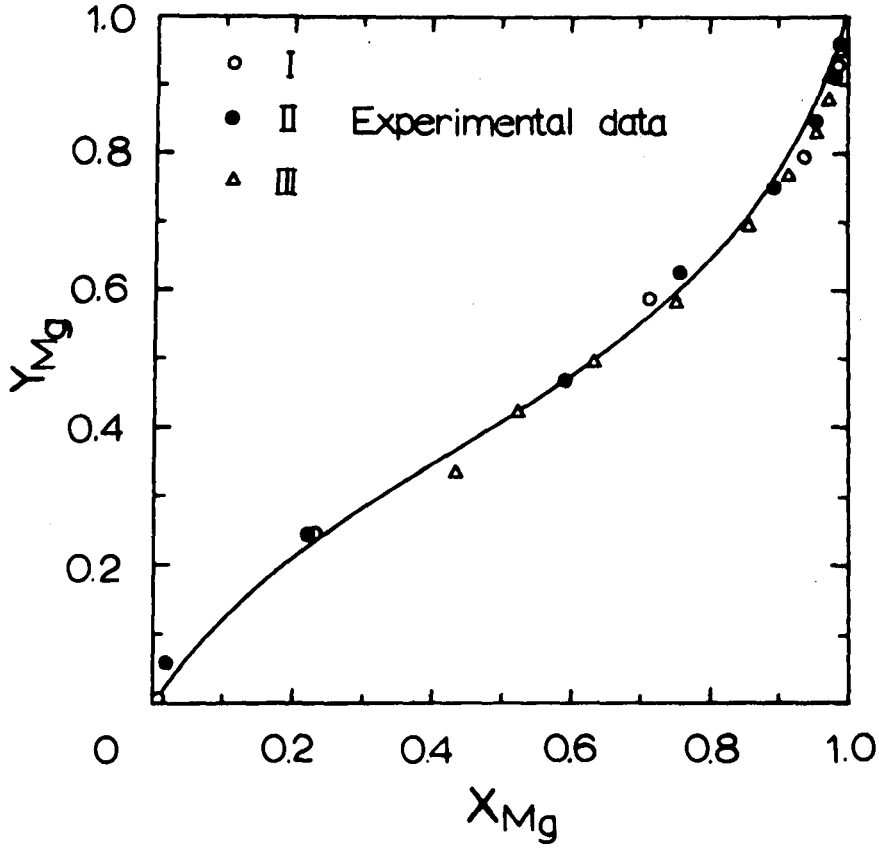

Figure 11. The normalized cation exchange isotherm of the Mg → Ca exchange for Hanford sandy loam soil with the modified Kielland function shown by the solid line.

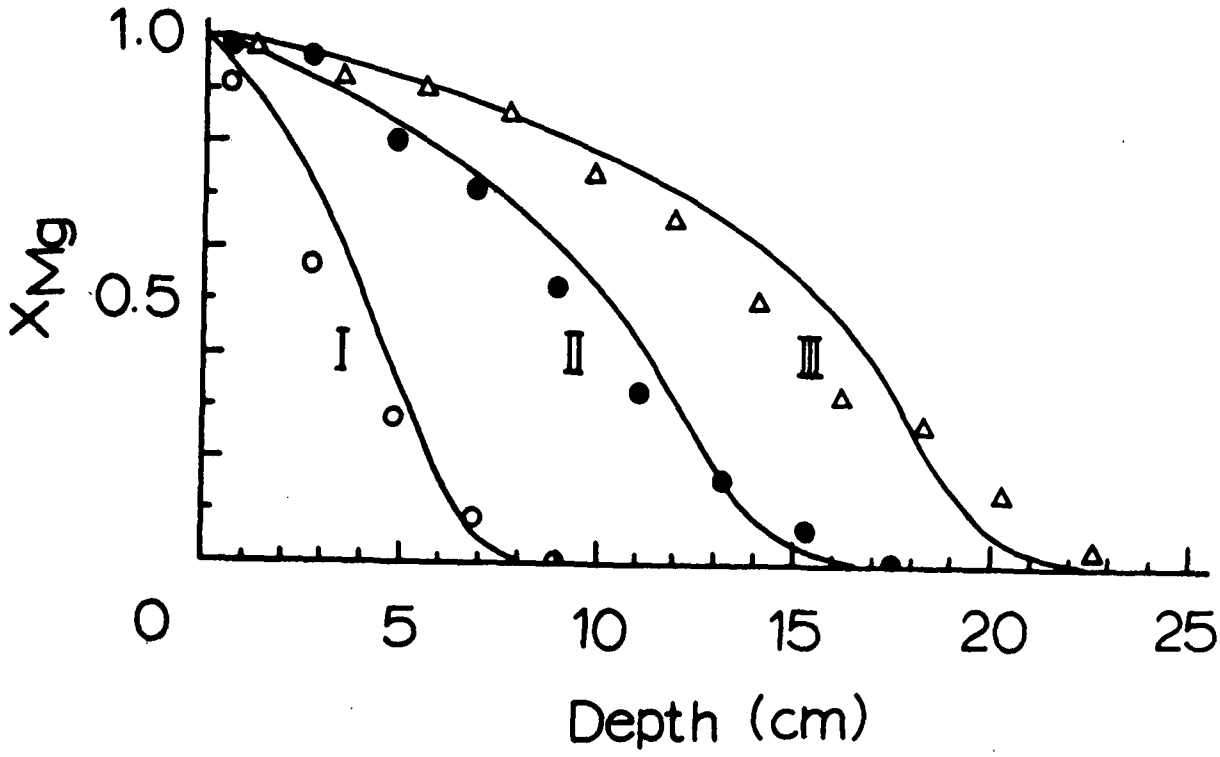

Figure 12. The normalized concentration profiles of the solution phase for three Nibley clay loam columns. The experimental values are represented by the points and the theoretically computed values by the lines.

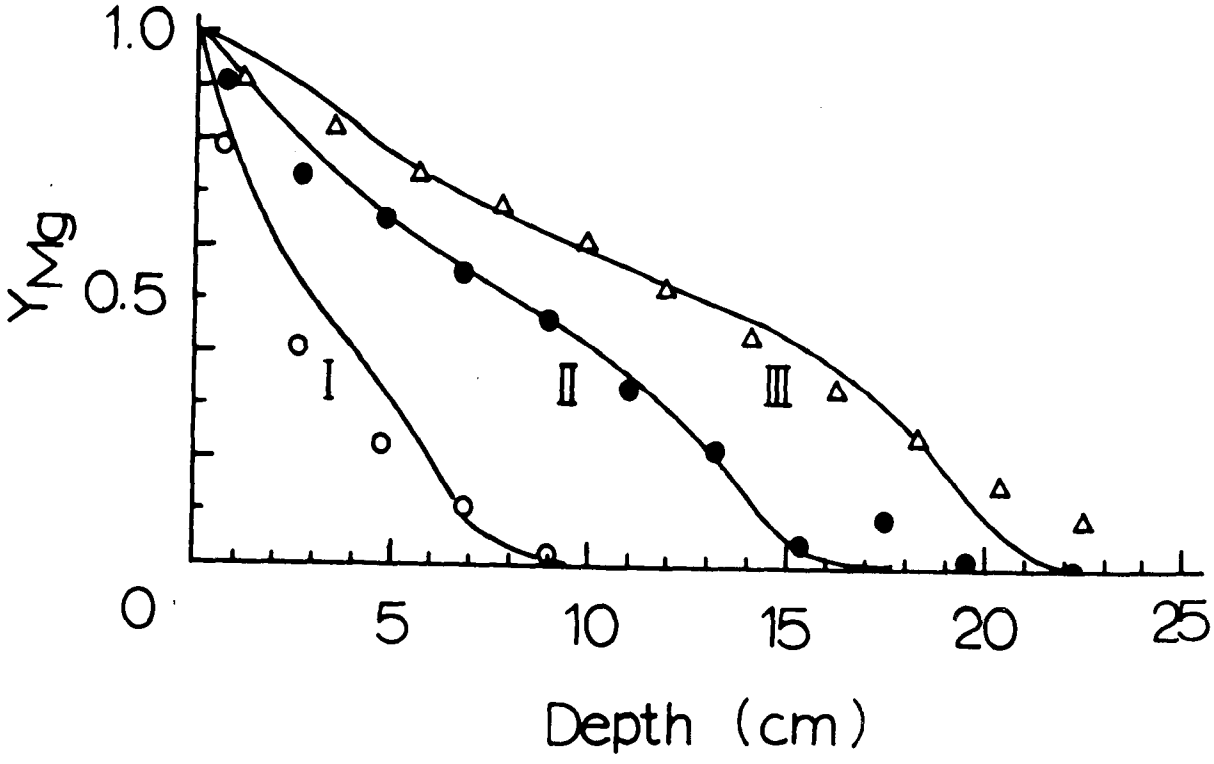

Figure 13. The normalized concentration profiles of the adsorbed phase for three Nibley clay loam columns. The experimental values are represented by the points and the theoretically computed values by the lines.

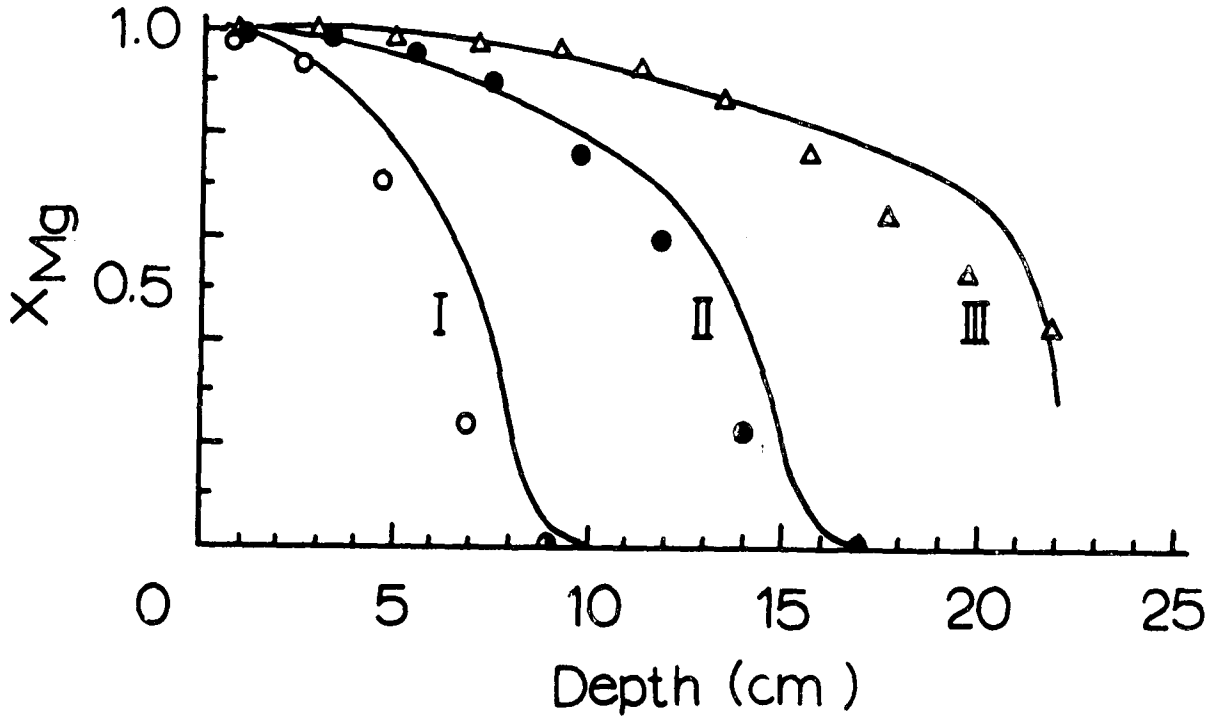

Figure 14. *The normalized concentration profiles of the solution phase for three Hanford sandy loam columns. The experimental values are represented by the points and the theoretically computed values by the lines.*

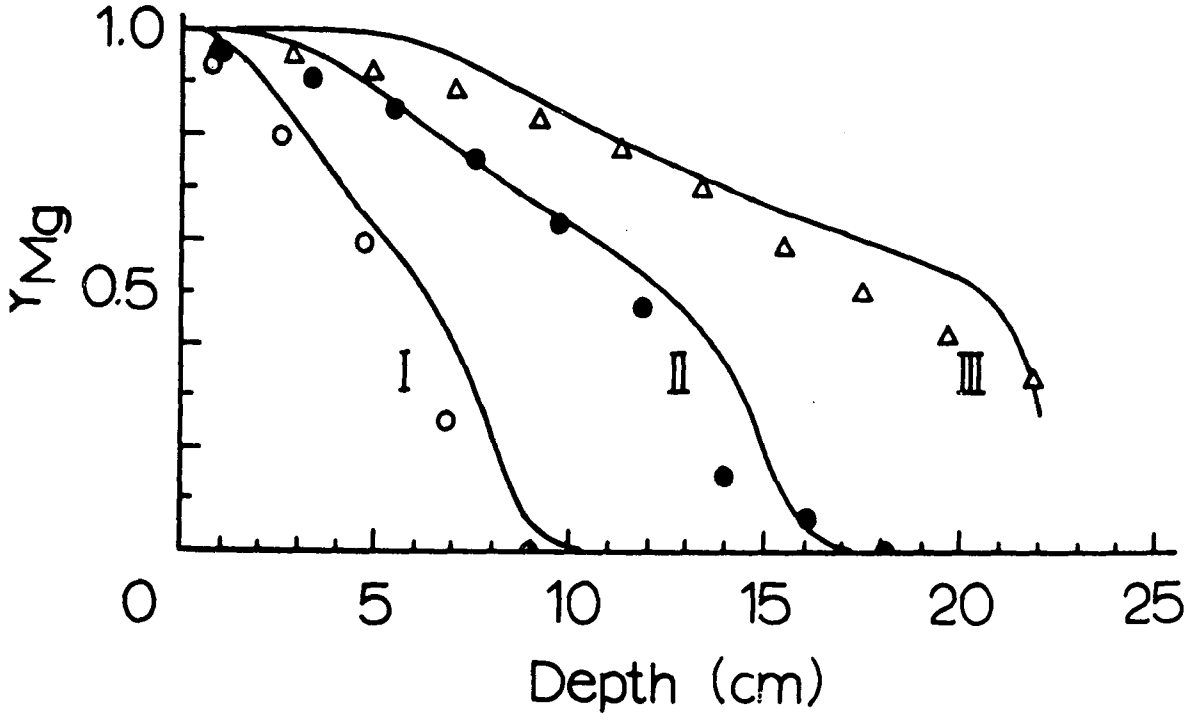

Figure 15. The normalized concentration profiles of the adsorbed phase for three Hanford sandy loam columns. The experimental values are represented by the points and the theoretically computed values by the lines.

made for the adsorbed phase profiles in Figure 15. The advanced front of the experimental profiles, the low concentration range, is more diffused than theoretically computed. This phenomenon, though less severe, was also observed in the Yolo and Nibley columns. At least two factors can contribute to this situation: (1) a non-equilibrium process between the solution phase and the exchanger phase during miscible displacement, (2) a change in the fluid dispersion during the cation displacement process. In the model developed, fluid dispersion is assumed constant and equal to the value determined by chloride displacement.

The second-order kinetics of cation exchange as expressed by Hiester and Vermuelen (1952) is

$$\frac{dS_A}{dt} = k[C_A (Q-S_A) - \frac{1}{K} S_A (C_o-C_A)] \qquad [16]$$

where k is the rate constant for adsorption, K is the exchange constant for the reaction, S_A is the amount of cation adsorbed per unit mass of exchanger and C_A is the concentration of the exchanging cation solution. The remaining variables have been defined earlier. At low concentrations where S_A and C_A are small, Equation [16] can be approximated by

$$\frac{dS_A}{dt} \simeq kC_AQ$$

Thus, the rate of cation exchange is a function of both the concentration of the exchanging cation, C_A, and the cation exchange capacity, Q, of the soil. Both Yolo loam and Nibley clay loam have Q values of about 25 me/100g while Hanford sandy loam has a Q value of about 6 me/100g. Comparison of these data allows the conclusion to be made that, at a

given value of C_A and k, the rate of exchange in he Hanford soil is significantly slower than in the other soils studied. Thus, the assumption of equilibrium conditions in the Hanford soil probably has a lower degree of validity than in the other soils. The study of Biggar and Nielsen (1963) using Oakley sand, with a Q value of 3.75 me/100 g, tends to corroborate the above conclusion. They showed that by varying the flow velocity from 1.77 cm/hr to 0.194 cm/hr the discrepancy between their experimental values and those predicted by the model of Lapidus and Amundson was significantly reduced in the region of $C/C_o = 0.5$. The slower flow rate allowed equilibrium to be more closely approximated, hence, compensating for the low Q value of their soil. Thus, at low concentrations of the exchanging cation, exchange equilibrium depends on both the flow velocity of the displacement process and the Q value (CEC) of the soil.

Although the value of the dispersion coefficient is assumed invariant during a miscible displacement experiment, the possibility exists that the value does vary. However, the degree of variation, if it does occur, is difficult to assess. The measurement of the dispersion coefficient before and after miscible displacement may provide an estimate of the degree of variability.

Application of the Nonlinear Model to Na → Ca Exchange

The nonlinear model was applied to the heterovalent system involving Na → Ca exchange. The soil used in the column study was Yolo loam. The experimental isotherm is given in Figure 16 and is classified as a Type II isotherm (See Figure 1). It was found that the general nonlinear exchange function expressed in Equation [12] did not describe the curve adequately. The function was modified, as shown by Lai

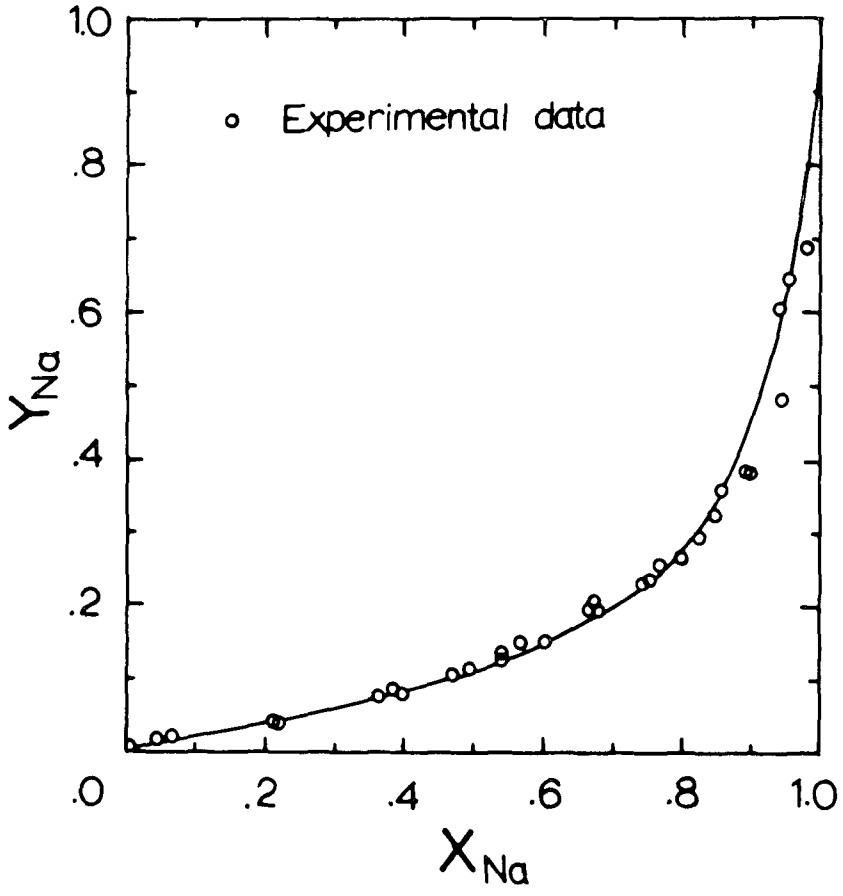

Figure 16. The reduced Na^+ adsorption isotherm in Yolo loam soil. The solid line is represented by Equation [17].

(1970), to yield an exchange function which is written

$$Y = \frac{X}{X + (1-X)\,[k' + C(1-2X)]} \qquad [17]$$

where k' and C were found to be 8.0 and -4.0, respectively, for the Na → Ca exchange. The modified exchange function is plotted as a solid line in Figure 16. The modification fit the data reasonably well. The modified exchange equation was used in solving the material balance equation. The numerical solution of the material balance equation along with the experimental data from three column experiments are given in terms of X(z, t) and Y(z, t) in Figures 17 and 18, respectively.

The sharp drop of the reduced concentration X at the profile front (Figure 17) predicted by theory was not obtained experimentally. This can be ascribed to the possibility that actual equilibrium was not reached throughout the column, thus, the cation was allowed to travel further down the soil column before it reached equilibrium with the exchanger phase. The result is a flatter profile at the advancing front of the soil solution.

The deviation from theory of the reduced concentration in the exchanger phase, Y(z, t) as shown in Figure 18, is not as marked. The reason is that at low concentrations of Na^+ in the percolating water, Y values are relatively low and change less with X.

In the column studies, it was noted that the flow velocity decreased as the amount of Na^+ ion solution introduced in the column increased. In the theoretical computation an overall average flow velocity was used. Hence, some of the deviation noted, in both Figures 17 and 18,

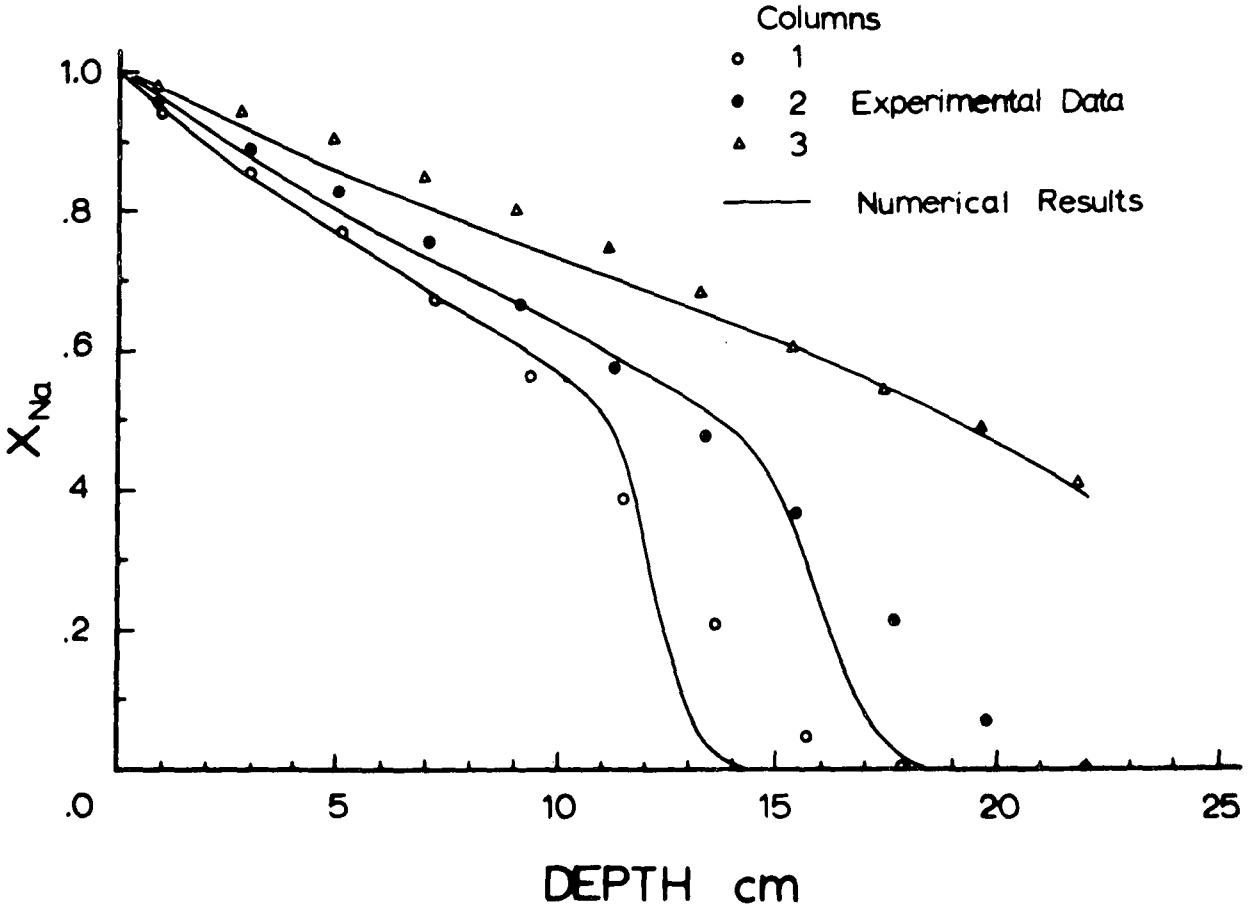

Figure 17. The concentration profiles $X_{Na}(z, t)$ for the three column experiments.

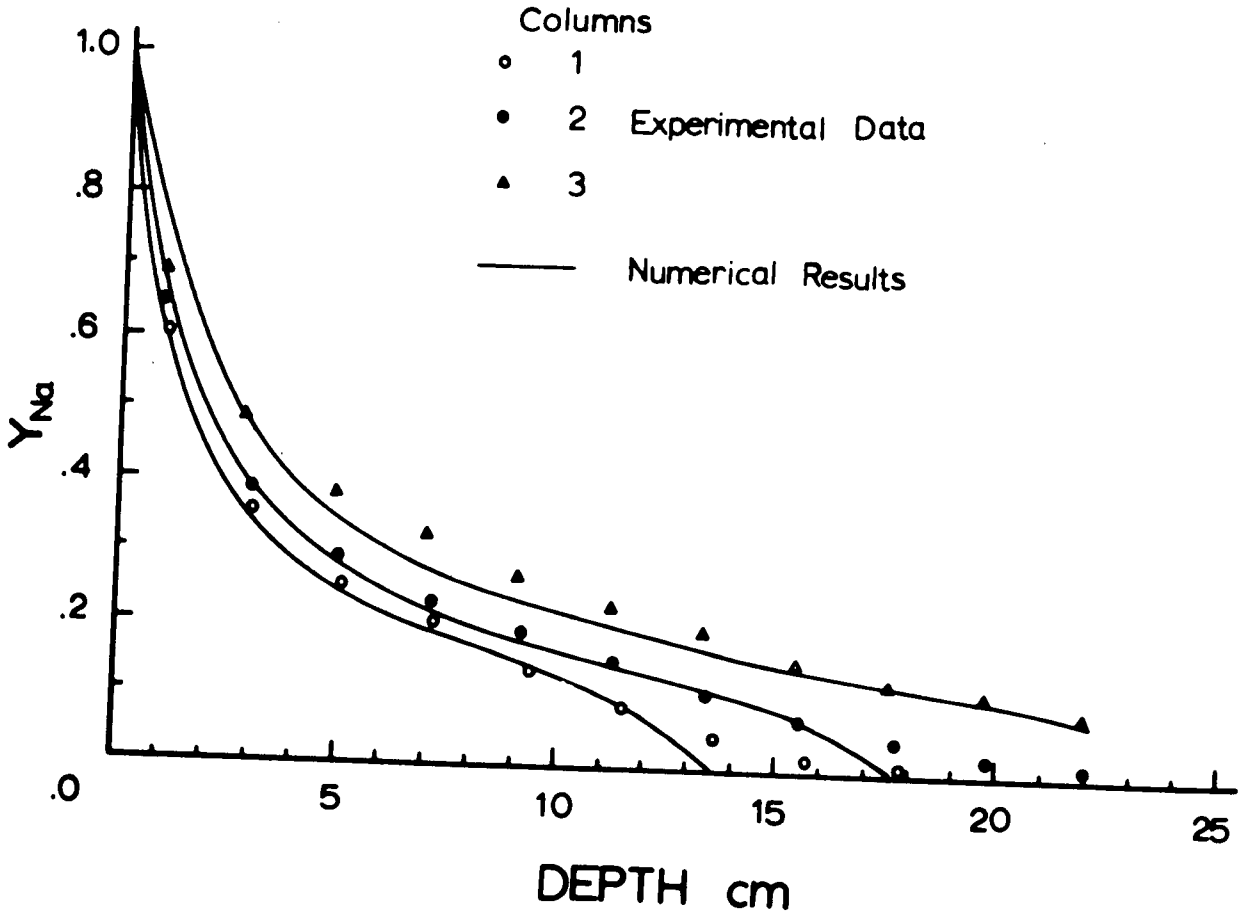

Figure 18. The concentration profiles $Y_{Na}(z, t)$ for the three column experiments.

from theory may be attributed to this factor. For the heterovalent system, the model developed in this study allowed reasonable prediction of cation transport.

PART B

MAGNESIUM ION EFFECT ON CARBONATE SOLUBILITY

SECTION VII

INTRODUCTION

The application of irrigation water to a soil can result in either the precipitation of carbonates from the water or the dissolution of existing carbonate material in the soil matrix by the water. Either of these reactions has a direct influence on the quality of water returning to the stream. The solution of calcium and magnesium carbonates not only affects the total salt load in the return flow, but also adds to the total hardness of the water. Eldridge (1960) considers, from the viewpoint of industrial and municipal pollution, the increase in water hardness to be the most important single adverse effect contributed by irrigation return flow to downstream use.

From agronomic considerations, carbonate precipitation, while reducing the total salt load of the water, increases the sodium hazard of return flow water by reducing the concentrations of Ca^{+2} and Mg^{+2} ions in relation to the Na^{+} ion. Eaton (1950) was one of the first to recognize the potential hazard and introduced the concept of residual sodium carbonate. This was an attempt to estimate the sodium hazard of the waters by assuming that all Ca^{+2} and Mg^{+2} ions precipitate in the presence of excess HCO_3^- and CO_3^{-2} ions. Recent studies (Bower, Ogata, and Tucker, 1968; Doner and Pratt, 1969) have placed more emphasis on the pertinent chemistry of calcium and magnesium carbonate systems and how it relates to carbonate precipitation from irrigation waters.

The effect of Mg^{+2} ion is of particular interest since both Ca^{+2} and Mg^{+2} are usually linearly combined in predictive precipitation equations (Eaton, 1970; Bower et al., 1968) whereas, their chemistry is not necessarily similar.

Davies (1962), Garrels and Christ (1965), and Nakayama (1968) have shown that Mg^{+2} and Ca^{+2} ions readily form ion-pairs. The effect of ion-pair formation on a $CaCO_3$ solution is to increase the amount of $CaCO_3$ which will dissolve and to decrease the amount which will precipitate as compared to a system without ion-pairs. The thermodynamic solubility product constant for $CaCO_3$ is still valid, but increasing $CaCO_3$ must dissolve to maintain a constant value for the ion activity product. While ion-pairs involving Ca^{+2}, HCO_3^-, and OH^- ions exist for waters in the absence of Mg^{+2} ion, the addition of Mg^{+2} ion results in increased ion-pair formation and, hence, increased solubility of $CaCO_3$. In addition to Mg ion-pairs, the Mg^{+2} ion may also affect $CaCO_3$ precipitation by inhibiting calcite nucleation.

The formation of a precipitate may be considered to consist of two distinct processes, nucleation and crystal growth. The fact that supersaturated solutions exist for definite periods of time suggests that the process of initiating precipitation (nucleation) differs from the process of continuing precipitation (crystal growth). Fisher (1962) states that the distinction between the two reactions results from the fact that in crystal growth the driving force is the difference in free energy between the ions in the crystal lattice and the hydrated ions in solution, while in nucleation no lattice and, hence, no lattice energy exists.

The effect of Mg^{+2} ion on $CaCO_3$ nucleation was first recognized by Leitmeier (1968) who found that Mg^{+2} ion favored the precipitation of aragonite over calcite (Bischoff, 1968). Doner and Pratt (1969) found the $CaCO_3$ precipitated and Mg was coprecipitated in the solid phase. Bischoff (1968) showed that Mg^{+2} ion inhibited the diagenetic aragonite to calcite transformation by reacting with the calcite nuclei. He

postulated that the strongly hydrated Mg^{+2} ion reduced the rate of growth of calcite nuclei because of the rate-controlling dehydration of the Mg^{+2} ion. After dehydration, however, the calcite lattice preferentially accepts the smaller Mg^{+2} ion. The inhibition to crystal transformation is overcome when sufficient calcite nuclei are present to reduce Mg^{+2} ion concentration to a level at which new nuclei can form which do not contain Mg^{+2} ion.

The Mg^{+2} ion can also affect carbonate equilibrium by interacting with the solid phase. Akin and Lagerwerff (1965) reported enhanced solubility of $CaCO_3$ precipitating from supersaturated solutions in the presence of Mg^{+2} and SO_4^{-2} ions. They developed a theory of enhanced carbonate solubility based on the surface adsorption of Mg^{+2} and SO_4^{-2} ions, and the constituent-ions of $CaCO_3$ on the crystal surface.

Weyl (1961) found that the slow kinetics of calcite dissolution in the presence of Ca^{+2} and Mg^{+2} ions could not be explained by ion-pair formation and concluded that the rate inhibiting mechanism was at the solid-liquid interface. Chave and Schmalz (1966) found, using pH-sensing techniques, that three factors (mineralogy, grain size, and character) involving the solid phase controlled the interaction of the carbonate crystal with the associated waters. They also found the activities of magnesium calcites were four times greater than pure calcite and that particles of calcite 10^{-6} cm in diameter have activities more than eight times greater than 1 cm particles.

This report represents the results of a study to define the role of Mg^{+2} ion in the precipitation and dissolution of carbonates in systems which contain excess solid carbonate.

SECTION VIII

MATERIALS AND METHODS

The studies consisted of equilibration of four series of artificial waters (see Table 4) with four solid carbonates and the determination of the amount of carbonate which dissolved or precipitated. Waters 1, 2, and 3 are undersaturated with respect to $CaCO_3$, while water 4 is supersaturated. The waters within each series were at constant Ca^{+2} and HCO_3^- concentration, constant ionic strength, but varied in Mg^{+2} ion concentration from 0 to 2×10^{-3} M. The waters were made from appropriate mixtures of NaCl, $NaHCO_3$, $CaCl_2$, and $MgCl_2$ solutions. Two liters of each water were prepared fresh for each replication. It was found that water 4, the supersaturated water, was stable for a period of up to 48 hours. This stability or lack of precipitation is a function of how supersaturated a water is, the greater the supersaturation the shorter the period of time before nucleation occurs (Pytkowicz, 1965).

The four solid carbonate materials were: Mallinckrodt reagent grade $CaCO_3$, lot TEJ (T), Purecal U (U) from the Wyandotte Chemical Corp., Millville loam soil, and Portneuf siltloam soil. T and U were shown by X-ray diffraction techniques to be calcite. Surface area measurements using stearic acid adsorption after the method of Suito et al. (1955) showed T to have a surface area of ~0.8 m^2/g and U to have a surface area of ~13.5 m^2/g.

Millville soil is a highly calcareous soil (~45% $CaCO_3$ equivalent) from Northeastern Utah. X-ray diffraction showed the calcareous material to be predominantly dolomite with a small amount of calcite present. Portneuf is a calcareous loess soil (20% $CaCO_3$ equivalent) from the Snake River Valley in Southwestern Idaho. X-ray diffraction showed

Table 4. Composition of the Four Waters Used in the "Carbonate Saturometer." Ionic Strength for all Waters was, I = .05

Waters		Ca^{+2}	HCO_3^-	Mg^{+2}
		Conc. M/liter		
1.	a	5×10^{-4}	5×10^{-4}	0
	b	5×10^{-4}	5×10^{-4}	5×10^{-5}
	c	5×10^{-4}	5×10^{-4}	2.5×10^{-4}
	d	5×10^{-4}	5×10^{-4}	5×10^{-4}
	e	5×10^{-4}	5×10^{-4}	1×10^{-3}
	f	5×10^{-4}	5×10^{-4}	2×10^{-3}
2.	a	5×10^{-4}	1×10^{-3}	0
	b	5×10^{-4}	1×10^{-3}	5×10^{-5}
	c	5×10^{-4}	1×10^{-3}	2.5×10^{-4}
	d	5×10^{-4}	1×10^{-3}	5×10^{-4}
	e	5×10^{-4}	1×10^{-3}	1×10^{-3}
	f	5×10^{-4}	1×10^{-3}	2×10^{-3}
3.	a	1×10^{-3}	1×10^{-3}	0
	b	1×10^{-3}	1×10^{-3}	5×10^{-5}
	c	1×10^{-3}	1×10^{-3}	2.5×10^{-4}
	d	1×10^{-3}	1×10^{-3}	5×10^{-4}
	e	1×10^{-3}	1×10^{-3}	1×10^{-3}
	f	1×10^{-3}	1×10^{-3}	2×10^{-3}
4.	a	2×10^{-3}	2×10^{-3}	0
	b	2×10^{-3}	2×10^{-3}	5×10^{-5}
	c	2×10^{-3}	2×10^{-3}	2.5×10^{-4}
	d	2×10^{-3}	2×10^{-3}	5×10^{-4}
	e	2×10^{-3}	2×10^{-3}	1×10^{-3}
	f	2×10^{-3}	2×10^{-3}	2×10^{-3}

the calcareous material to contain about equal amounts of calcite and dolomite. Approximately 0.25 g of $CaCO_3$ or 1 g of soil was equilibrated with 100 ml of solution. Equilibrium was determined when a constant pH value was obtained.

SECTION IX

THE CARBONATE SATUROMETER

Any determination of carbonate solubility is complicated by the number of system variables which cannot be experimentally measured. Attempts to use the thermodynamic-derived constants for various equilibria require that corrections be made for ion-pair formation, the ionic strength and the deviation of the solid phase from its standard state of unit activity.

To overcome these difficulties the "carbonate saturometer" method, as developed by Weyl (1961) was used to measure carbonate solubility. This method is based upon the fact that the pH of a solution changes when the CO_3^{-2} ion is added or removed from solution. The reactions involved are:

$$HCO_3^- \rightleftarrows H^+ + CO_3^{-2} \qquad [1]$$

$$Ca^{+2} + CO_3^{-2} \rightleftarrows CaCO_3 \ (s) \qquad [2]$$

$$Ca^{+2} + HCO_3^- \rightleftarrows H^+ + CaCO_3 \ (s) \qquad [3]$$

If the water is undersaturated with respect to a solid carbonate, the carbonate dissolves, yielding CO_3^{-2} ions which combine with H^+ ions, thereby increasing the pH of the solution. If the water is supersaturated with respect to a solid carbonate, the carbonate precipitates, HCO_3^- ions dissociate, the pH decreases. If the water is saturated with respect to a solid carbonate, the pH of the suspension remains the same.

The "carbonate saturometer" is calibrated for each water by comparing the amounts of strong acid (+Z) or base (-Z) required to produce the

same ΔpH as was produced by a standard addition of y' moles of bicarbonate. The calibration results in:

$$F(x) = -Z/y' \qquad [4]$$

where F(x) is a function of apparent equilibrium constants, the hydrogen ion activity, and can be shown (Garrels and Christ, 1965) to be equal to:

$$F(x) = \frac{1 + 2K_2'/x}{1 + x/K_1' + K_2'/x} - 1 \qquad [5]$$

where x is the hydrogen ion activity, K_1' and K_2' are apparent equilibrium constants defined as:

$$K_1' = \frac{x(HCO_3^-)}{(H_2CO_3) + (CO_2)} \qquad [6]$$

$$K_2' = \frac{x(CO_3^{-2})}{(HCO_3^-)} \qquad [7]$$

where the parentheses represent concentrations of the various ionic species. Once this function is determined, the amount of carbonate y precipitated can be calculated from:

$$-y = Z/[1 - F(x)] \qquad [8]$$

where Z is the amount of strong acid (+Z) or base (-Z) required to produce the same ΔpH as resulted upon equilibration of the water with the solid carbonate. Approximately 0.001 N NaOH and HCl is used to calibrate the waters.

A Heath pH recording electrometer Model EU-301-A was used to obtain the necessary ΔpH measurements. The accuracy of the instrument was found to be better than 0.5% full scale (less than 0.01 pH on a recorder span of 2 pH units). All measurements were made in a reaction vessel (Figure 19) using a calomel reference electrode and a Corning glass electrode system. The equilibrium pH data were obtained at room temperature (22° C) with the water at equilibrium with atmospheric CO_2.

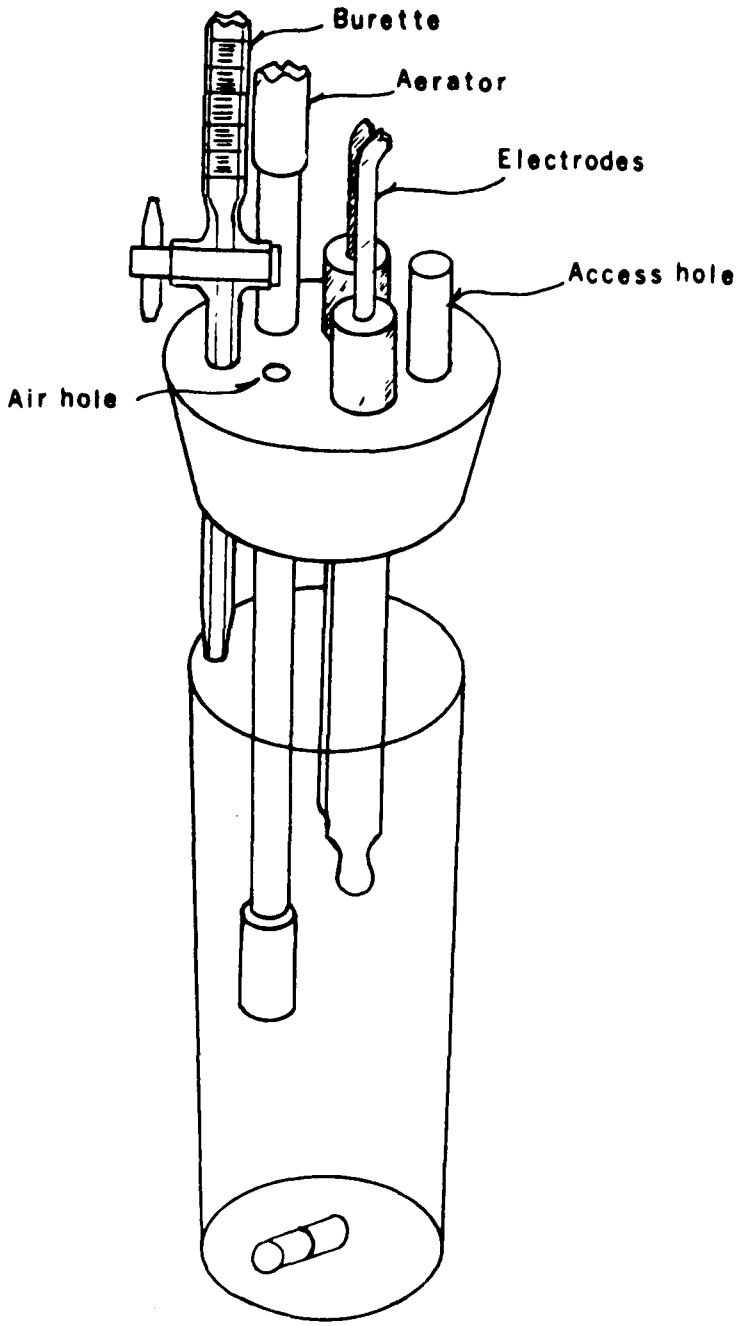

Figure 19. Reaction vessel of carbonate saturometer.

SECTION X

EXPERIMENTAL TECHNIQUE

The description of the experimental method using the carbonate saturometer is given. A 100 ml sample of a given water is pipetted into the reaction vessel (see Figure 19) and aerated until a constant pH is reached. The atmosphere above the water is flushed with N_2 gas and a slight positive pressure gradient of N_2 between the reaction vessel and the atmosphere is established. The water is titrated by adding 0.25 ml increments of approximately 2×10^{-3} N NaOH or HCl. The pH resulting from the addition of each increment is recorded. The titration curve which results is plotted as equivalents per liter vs pH.

A 100 ml subsample is taken from the same water sample and placed into the reaction vessel and aerated to constant pH. As aeration is continued, 0.5 ml increments of 1.0×10^{-2} M $NaHCO_3$ is added to samples which are undersaturated with respect to calcium carbonate or 0.5 ml increments of 1.0×10^{-1} M $NaHCO_3$ is added to samples which are supersaturated with calcium carbonate. The pH is allowed to stabilize between additions of the $NaHCO_3$ solutions. From the initial acid or base titration curve the equivalents of titer required to produce the same pH value that resulted from the addition of each increment of bicarbonate is determined. From Equation [4], F(x) is calculated for the water.

Another 100 ml subsample of water is taken and aerated to constant pH. An excess (1 - 2 grams) of solid $CaCO_3$ is added and the system aerated to constant pH. From the initial acid or base titration data the equivalents of titer required to produce the same pH value which resulted from the addition of solid $CaCO_3$ is determined. The amount

of carbonate precipitated or dissolved, -y or +y, respectively, is then calculated using Equation [8].

SECTION XI

RESULTS AND DISCUSSION

The results of the "carbonate saturometer" studies are given in Figures 20 to 23. The dissolution of solid carbonate in each water is plotted against the molar concentration of Mg^{+2} in the water. Positive values of Y are obtained when carbonate dissolves in the water, and negative values of Y indicate precipitation of carbonate. Each data point is the average of at least three replications. The lines drawn and the equations given are the result of linear regression analysis.

Figure 20 shows the data obtained when calcite T was equilibrated with the four waters. In all waters except water 3, the solubility of calcite increased as the Mg^{+2} ion concentration increased. The effect of Mg^{+2} in water 3 indicated no change or a slight decrease in solubility. The general trend in carbonate solubility can be ascribed to increased ion-pair formation promoted by Mg^{+2}, although the modified lattice concept of calcite solubility as proposed by Akin and Lagerwerff (1965) cannot be precluded. Where precipitation occurred (water 4) the increase in carbonate solubility corroborates the findings of Doner and Pratt (1969).

Figure 21 shows the same study using calcite U as the solid phase. It is noted that the solubility of calcite U (13.5 m^2/g) is generally higher in all waters than the solubility of calcite T (0.8 m^2/g). These data show the effect of surface area on calcite solubility and suggest the possibility that calcite U is in a metastable phase. This supports the conclusion of Chave and Schmalz (1966) who related carbonate solubility with particle size. The solubility of calcite U, when equilibrated

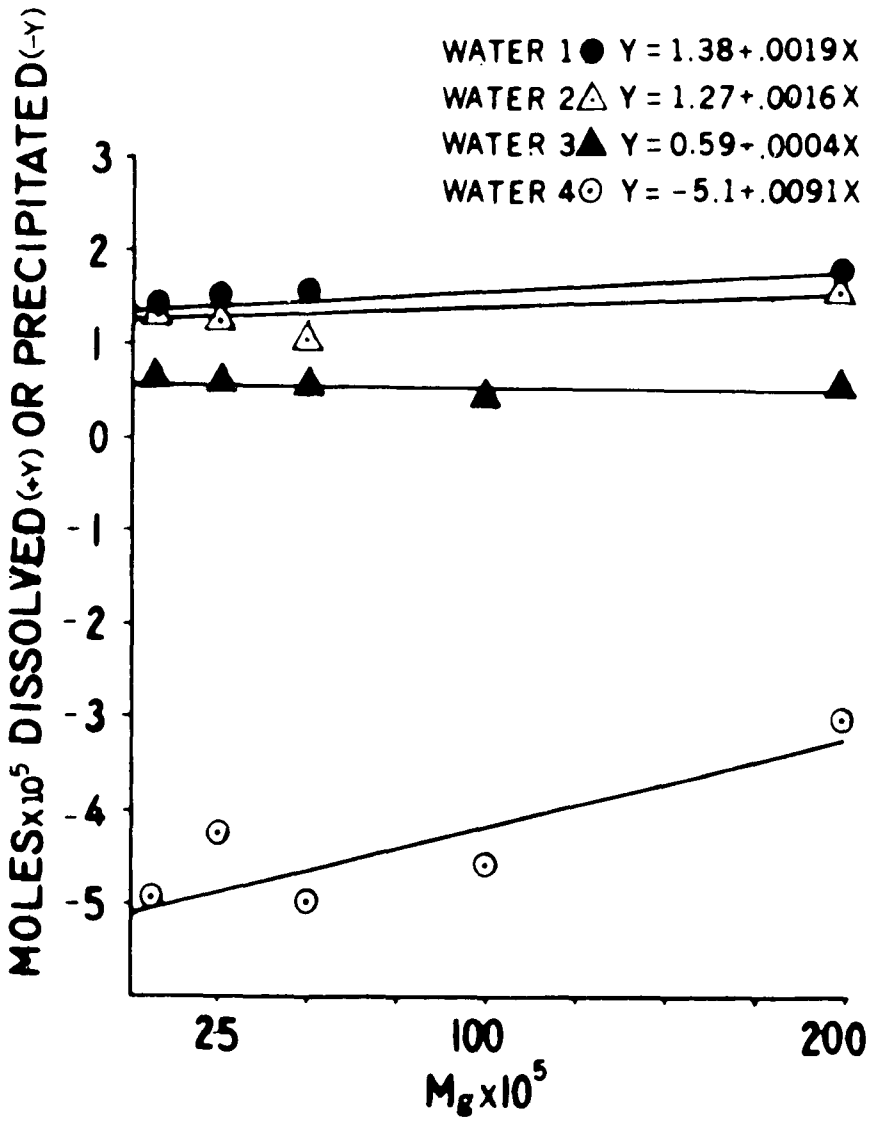

Figure 20. Amount of carbonate dissolved or precipitated upon equilibration of reagent grade calcite (T) with waters containing variable amounts of Mg^{+2}, in moles.

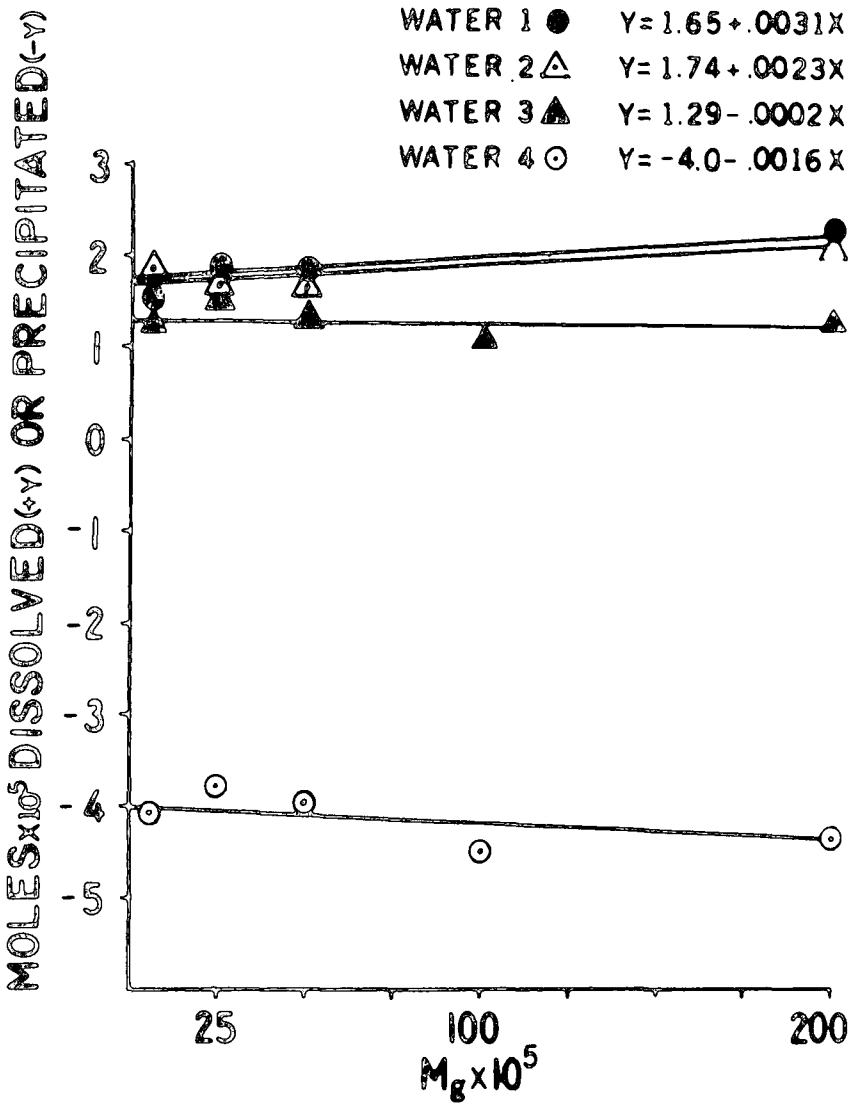

Figure 21. Amount of carbonate dissolved or precipitated upon equilibration of Purecal U (U) with waters containing variable amounts of Mg^{+2}, in moles.

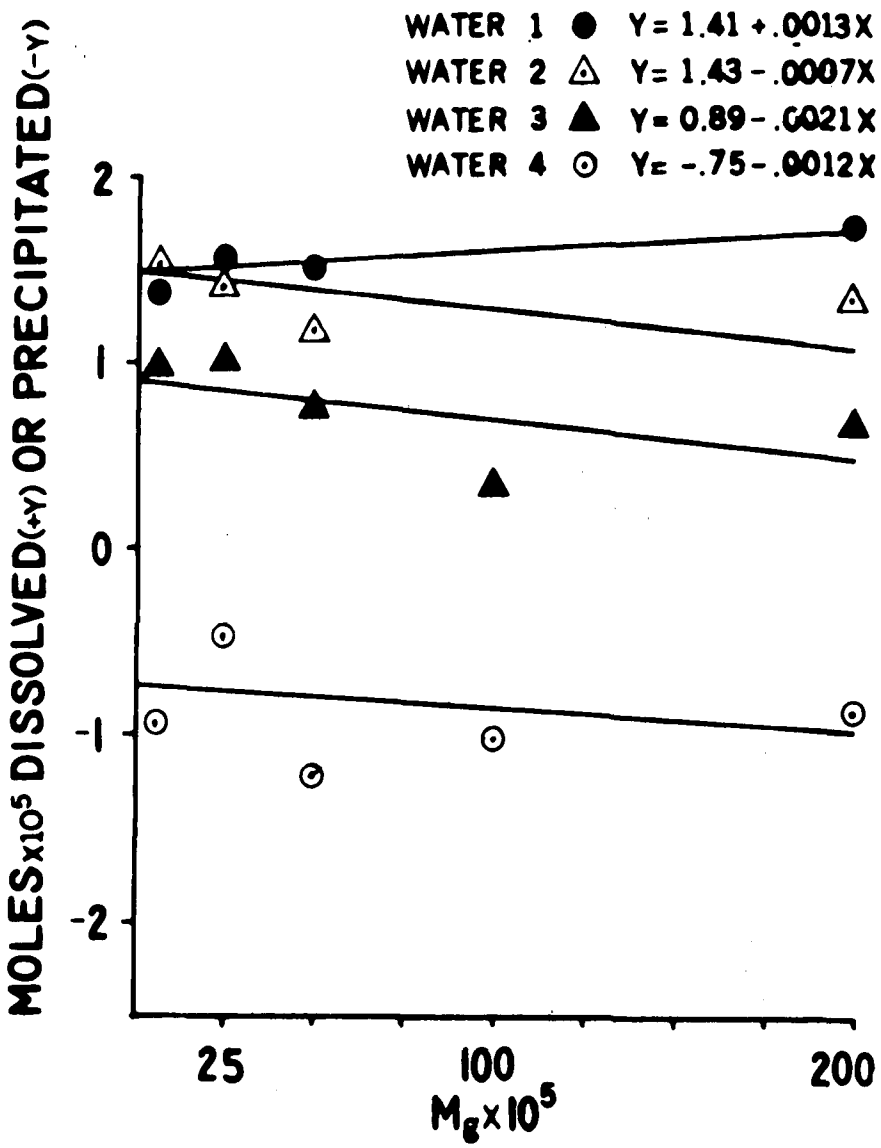

Figure 22. Amount of carbonate dissolved or precipitated upon equilibration of Portneuf soil with waters containing variable amounts of Mg^{+2}, in moles.

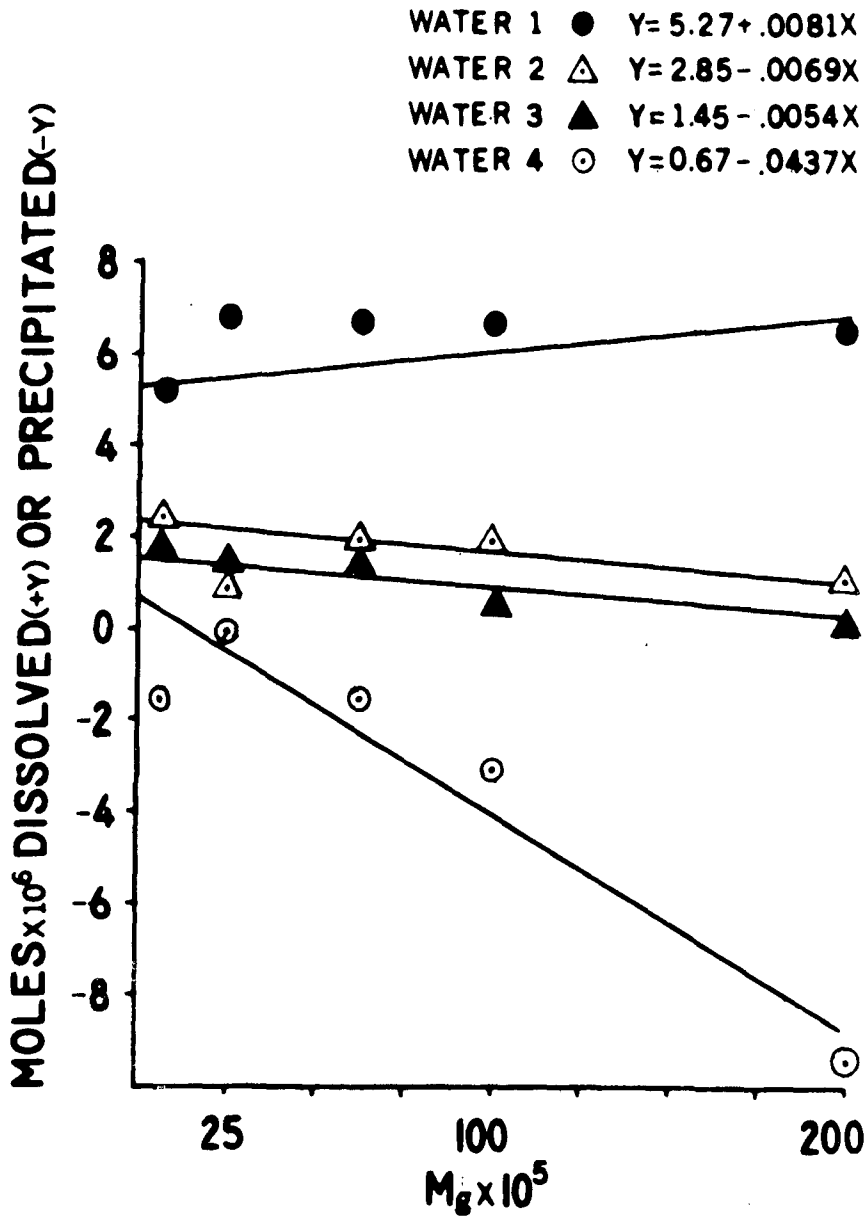

Figure 23. Amount of carbonate dissolved or precipitated upon equilibration of Millville soil with waters containing variable amounts of Mg^{+2}, in moles.

with undersaturated waters, followed the same pattern as did calcite T. However, when calcite U was equilibrated with supersaturated water 4, Mg^{+2} had no apparent effect on its solubility. The slight negative slope of the regression line is not considered significant. Thus, the type of calcite used in this study appears to affect its relationship with Mg^{+2}. The major difference found between the two calcite sources is that the specific area of calcite U is 17 times greater than the specific area of calcite T. This difference is reflected in the fact that the solubility of U is greater than T in water 4, when no Mg^{+2} is present. The data from the supersaturated system (Figure 21, water 4) suggest that, in the presence of an excessive number of possible nucleation sites, the precipitation of carbonate effectively removed Mg^{+2} from solution and incorporated it into the newly formed carbonate that had a Ca/Mg mole ratio of sufficient magnitude to stabilize the solubility of calcite U (Doner and Pratt, 1969). The relatively high concentration of Ca^{+2} in this system strengthens the possibility of maintaining a high Ca/Mg mole ratio in the precipitated phase. The removal of Mg^{+2} from solution also nullifies its ion-pair formation capabilities. This study infers that increasing the amount of nucleating surface essentially acts as a dilutent for Mg^{+2} and is a factor in determining the solubility of $CaCO_3$ precipitated from solution.

Figures 22 and 23 show how Mg^{+2} ion concentration in water varies the carbonate solubility in two calcareous soils. The Portneuf soil contains about equal amounts of dolomite and calcite, while the Millville soil is predominantly dolomite. When the soils were equilibrated with water 1, they behave similar to the calcite material T and U, i.e., the presence of Mg^{+2} increased the dissolution of solid carbonates in the soil. Upon equilibration of the Portneuf and Millville soils with undersaturated waters 2 and 3, the solubility of soil carbonates

decreased as the Mg^{+2} ion concentration was increased. These data are readily explained by the degree of saturation of waters. Water 1 is sufficiently undersaturated with respect to the carbonates in the soils that increasing the Mg^{+2} ion concentration only resulted in additional ion-pairs being formed, thus, increasing the solubility of the soil carbonates. Waters 2 and 3 are closer to saturation; hence, increasing the initial amount of Mg^{+2} ion resulted in a decrease in solubility due to the common effect of Mg^{+2} on the dolomite present in the soils. The common ion effect can also be used to explain the increase in precipitation noted when the soils are equilibrated with the supersaturated water.

SECTION XII

REFERENCES

1. Akin, G. W., and J. V. Lagerwerff. 1965. Calcium carbonate equilibria in solutions open to the air. IL Enhanced solubility of $CaCO_3$ in the presence of Mg^{+2} and SO_4^{-}. Geochimica et Cosmochimica Acta 29:253-360.

2. Biggar, J. W., and D. R. Nielsen. 1963. Miscible displacement: V. Exchange processes. Soil Science Society of America Proceedings 27:623-627.

3. Biggar, J. W., D. R. Nielsen, and K. K. Tanji. 1966. Comparison of computed and experimentally measured ion concentrations in soil column effluents. Transactions American Society of Agricultural Engineers 9:784-787.

4. Bischoff, J. L. 1968. Kinetics of calcite nucleation, magnesium ion inhibition and ionic strength catalysis. Journal of Geophysical Research 73:3315-3322.

5. Bower, C. A., G. Ogato, and J. M. Tucker. 1968. Sodium hazard of irrigation waters as influenced by leaching fraction and by precipitation or solution of calcium carbonate. Journal of Soil Science 106:29-34.

6. Bredehoeft, J. D. 1971. Comment on 'Numerical solution to the convective diffusion equation' by C. A. Oster, J. C. Sonnichsen, and R. T. Jaske. Water Resource Research 7:755-756.

7. Brenner, H. 1962. The diffusion model of longitudinal mixing in beds of finite length. Numerical values. Chemical Engineering Science 17:229-243.

8. Chave, K. E., and R. F. Schmalz. 1966. Carbonate-seawater interactions. Geochimica et Cosmochimica Acta 30:1037-1048.

9. Davies, C. W. 1962. Ion Association. Butterworths, London. 190 p.

10. Doner, H. E., and P. F. Pratt. 1969. Solubility of calcium carbonate precipitated in aqueous solutions of magnesium and sulfate salts. Soil Science Society of America Proceedings 33:690-693.

11. Dutt, G. R., and K. K. Tanji. 1962. Predicting concentrations of solutes in water percolated through a column of soil. Journal of Geophysical Research 67:3437-3439.

12. Eaton, F. M. 1950. Significance of carbonates in irrigation waters. Soil Science 69:123-133.

13. Eldridge, E. R. 1960. Return irrigation waters characteristics and effects. U. S. Department of Health, Education and Welfare, Region IX, Portland, Oregon, May.

14. Fisher, R. B. 1962. Surface of precipitated particles. Record of Chemical Progress 23:93-103.

15. Garrels, R. M., and C. L. Christ. 1965. Solutions, Minerals and Equilibria. Harper & Row, New York. p. 93-122.

16. Hashimoto, I., K. B. Deshpande, and H. C. Thomas. 1964. Peclet numbers and retardation factors for ion exchange columns. Industrial and Engineering Chemistry Fundamentals 3:213-218.

17. Helfferich, F. 1962. Ion Exchange. McGraw-Hill, New York.

18. Niester, N. K., and T. Vermeulen. 1952. Saturation performance of ion-exchange and adsorption columns. Chemical Engineering Progress 48:505-516.

19. Lai, Sung-Ho. 1970. Cation exchange and transport in soil columns undergoing miscible displacement. PhD Dissertation, Utah State University, Logan, Utah.

20. Lapidus, L., and N. R. Amundson. 1952. Mathematics of adsorption in beds. VI. The effect of longitudinal diffusion in ion-exchange and chromatographic columns. Journal of Physical Chemistry 56:984-988.

21. Leitmeier, H. 1968. Die absatze des minerolwasers rohitsch-saverbrunn steiermark. Cited by Bishoff, J. L. Journal of Geophysical Research 73:3315-3322.

22. Lindstrom, F. T., R. Haque, V. H. Freed, and L. Boersma. 1967. Theory on the movement of some herbicides in soils. Linear diffusion and convection of chemicals in soils. Environmental Science and Technology 1:561-565.

23. Nakayama, K. S. 1968. Calcium activity, complex and ion-pair in saturated $CaCO_3$ solution. Soil Science 106:429-434.

24. Oster, C. A., J. C. Sonnichsen, and R. T. Jaske. 1970. Numerical solution to the convective diffusion equation. Water Resource Research 6:1746-1752.

25. Oster, C. A. 1971. Reply. Water Resource Research 7:757.

26. Pinder, G. F., and H. H. Cooper, Jr. 1970. A numerical technique for calculating the transient position of the salt water front. Water Resource Research 6:875-882.

27. Pytkowicz, R. M. 1965. Rates of inorganic calcium carbonate nucleation. Science 146:196-199.

28. Rachinskii, V. V. 1965. The General Theory of Sorption Dynamics and Chromatography. Translation from Russian. Consultants Bureau. New York.

29. Rifai, M. N. E., W. J. Kaufman, and D. K. Todd. 1956. Dispersion phenomena in laminar flow through porous media. Report No. 3, Industrial Engineering Report Series 90, Sanitary Engineering Research Lab, University of California, Berkeley.

30. Suito, E., A. Masafumi, and T. Arakawa. 1955. Surface area measurement of powder by adsorption in liquid phase (L). Bulletin of the Institute of Chemical Research, Kyto, University, Japan, 33:1-7.

31. Weyl, P. K. 1961. The carbonate saturometer. Journal of Geology 69:32-44.

SECTION XIII

PUBLICATIONS AND PATENTS

1. Hassett, J. J. 1970. Magnesium ion inhibition of calcium carbonate precipitation and its relations to water quality. PhD Dissertation, Utah State University, Logan, Utah.

2. Hassett, J. J., and J. J. Jurinak. 1971. Effect of Mg^{+2} ion on the solubility of solid carbonates. Soil Science Society of America Proceedings 35:403-406.

3. Hassett, J. J., and J. J. Jurinak. 1971. Effect of ion-pair formation on calcium and magnesium ion activities in aqueous carbonate solutions. Soil Science 111:91-94.

4. Lai, Sung-Ho. 1970. Cation exchange and transport in soil columns undergoing miscible displacement. PhD Dissertation, Utah State University, Logan, Utah.

5. Lai, Sung-Ho, and J. J. Jurinak. 1972. One dimensional cation saturation performance in a steady state flow through a soil column: A numerical approach. Water Resources Research 8:99-107.

6. Lai, Sung-Ho, and J. J. Jurinak. 1971. Numerical approximation of cation exchange in miscible displacement through soil columns. Soil Science Society of America Proceedings 35:894-899.

7. Lai, Sung-Ho, and J. J. Jurinak. 1972. The transport of cations in soil columns at different pore velocities. Soil Science Society of America Proceedings 36:730-733.

SECTION XIV

APPENDIX

I. The FORTRAN program to solve the Equations [10] through [11], by the explicit method with a "Kielland" type exchange function.

```
C.....................................................................
C
C   PURPOSE
C      TO SOLVE THE MATERIAL BALANCE EQUATION, WHICH IS THE INITIAL
C      BOUNDARY VALUE PROBLEM THAT GOVERNS THE CATION TRANSPORT
C      PROCESS IN THE STEADY DISPLACEMENT FLOW.
C
C   DESCRIPTION OF PARAMETERS
C      IDSET      NUMBER OF DATA SET
C      SIGN       DATA SET IDENTIFICATION AN ALPHANUMERIC
C                 ARRAY
C      D          DISPERSION COEFFICIENT
C      V          INTERSTITIAL FLOW VELOCITY
C      RO         BULK DENSITY
C      Q          CATION EXCHANGE CAPACITY
C      ALF        PORE FRACTION
C      CO         TOTAL CONCENTRATION
C      HZ         DEPTH INCREMENT
C      HT         TIME INCREMENT
C      IT         OUTPUT CONTROL NUMBER
C      IZ         OUTPUT CONTROL NUMBER
C      N          TOTAL NUMBER OF THE DEPTH INCREMENT
C      MT         TOTAL NUMBER OF THE TIME INCREMENT
C      C          CONSTANT IN KIELLAND FUNCTION
C      ALNK       CONSTANT IN KIELLAND FUNCTION
C      T          TIME
C      X          SOLUTION CONCENTRATION AN ARRAY
C      YOX        EXCHANGER CONCENTRATION  AN ARRAY
C
C   INPUT
C      SIGN
C      D,V,RO,Q,ALF,CO
C      HZ,HT,MT,N,IT,IZ
C      C,ALNK
C
C   OUTPUT
C      SIGN
C      D,V,RO,Q,ALF,CO
C      HZ,HT
C      C,ALNK
C      T,X(I)
C      YOX(I)
```

```
C
C   SUBROUTINE REQUIRED
C      EXFCN
C
C   METHOD
C      AN EXPLICIT METHOD DESCRIBED IN THE TEXT
C
C.....................................................................
C   MAIN PROGRAM
C
       DIMENSION X(100), Y(100), YOX(100), SIGN(11)
       IDSET = 2
       DO 10 ID = 1, IDSET
C
C   INPUT OF BASIC DATA
C
       READ(5,99) (SIGN(I), I = 1,11)
       WRITE(6,199)(SIGN(I), I = 1,11)
       READ(5,100) D,V,RO,Q,ALF,CO
       READ(5,101) HZ,HT,MT,N,IT,IZ
       WRITE(6,200) D,V,RO,Q,ALF,CO
       WRITE(6,201) HZ,HT
       NP1 = N + 1
       NM1 = N - 1
       DZ2 = D/(HZ*HZ)
       VZ = V/(2.*HZ)
       RQAC = (RO*Q)/(ALF*CO)
       READ(5,102)C, ALNK
       WRITE(6,202)C, ALNK
C
C   SET THE TOP BOUNDARY AND INITIAL CONDITIONS
C
       X(1) = 1.0
       DO 1 I = 2, NP1
     1 X(I) = 0.0
       KN = 0
       T = 0.0
C
C   BEGIN THE COMPUTATION OF X(I)
C
       DO 20 IIT = 1, MT
       DO 30 I = 2, N
       EOX = EXP(ALNK + C*(1. - 2.*X(I)))
       FOX = ((1. + 2.*C*X(I)*(1. - X(I)))*EOX)/((X(I) +
      &(1. - X(I))*EOX)**2)
       FT = (1. + RQAC*FOX)/HT
       Y(I) = ((DZ2 - VZ)*X(I + 1) - (2.*DZ2 - FT)*X(I) +
      &(DZ2 + VZ)*X(I - 1))/FT
    30 CONTINUE
```

```
C
C   EVALUATE THE BOTTOM BOUNDARY
C
      Y(NP1) = Y(NM1)
      DO 40 J = 2, NP1
   40 X(J) = Y(J)
      KN = KN + 1
      T = T + HT
      IF(KN.NE.IT) GO TO 20
C
C     OUTPUT X(I)
C
      WRITE(6,203) T, (X(I), I = 1, N, IZ)
C
C   COMPUTE YOX(I) IN SUBROUTINE EXFCN
C
      CALL EXFCN(X, C, ALNK, N, YOX)
C
C   OUTPUT YOX(I)
C
      WRITE(6,204) (YOX(I), I = 1, N)
      KN = 0
   20 CONTINUE
   10 CONTINUE
C
   99 FORMAT(11A4)
  100 FORMAT(6F10.4)
  101 FORMAT(2F10.4, 4I5)
  102 FORMAT(2F10.5)
  199 FORMAT(1H1, 10X, 11A4)
  200 FORMAT(1H1, 14X, 'DISPERSION COEFFICIENT', F15.6/15X,
     &'FLOW VELOCITY',F15.6/15X,'BULK DENSITY', F15.6/15X,
     &'EXCHANGE CAPACITY', F15.6/15X, 'PORE FRACTION', F15.6
     &/15X, 'TOTAL CONCENTRATION', F15.6)
  201 FORMAT (//14X, 'DEPTH INTERVAL',F15.6, 10X, 'TIME
     &INTERVAL', F15.6)
  202 FORMAT(1H1, 13X, 'CONSTANT C IS', F10.6, 'CONSTANT
     &LN K IS', F10.6//)
  203 FORMAT(1H , 14X, 'TIME IS', F10.2//(10F13.7))
  204 FORMAT(//(10F13.7))
      STOP
      END
```

```
C.....................................................................
C
C   SUBROUTINE EXFCN
C
C   PURPOSE
C      TO EVALUATE Y(I) AS A FUNCTION OF X(I)
C
C   USAGE
C      CALL EXFCN(X, C, ALNK, N, YOX)
C
C.....................................................................
C

      SUBROUTINE EXFCN(X, C, ALNK, N, YOX)
      DIMENSION X(100), YOX(100)
      DO 1 I = 1, N
    1 YOX(I) = X(I)/(X(I) + (1. - X(I))*EXP(ALNK + C*(1. -
     &2.*X(I))))
      RETURN
      END
```

II. The FORTRAN program to solve the Equations [10] through [11] with a linear exchange isotherm.

```
C.....................................................................
C
C    PURPOSE
C       TO SOLVE THE MATERIAL BALANCE EQUATION THAT GOVERNS
C       THE CATION TRANSPORT WITH A LINEAR CATION EXCHANGE
C       FUNCTION
C
C    DESCRIPTION OF PARAMETERS
C       D          DISPERSION COEFFICIENT
C       V          FLOW VELOCITY
C       RO         BULK DENSITY
C       Q          EXCHANGE CAPACITY
C       ALF        PORE FRACTION
C       CO         TOTAL CONCENTRATION
C       HZ         DEPTH INCREMENT
C       HT         TIME INCREMENT
C       MT         NUMBER OF TIME INCREMENT
C       N          NUMBER OF THE DEPTH INCREMENT
C       SLOPE      THE CONSTANT OF THE EXCHANGE FUNCTION
C       AINCP      THE CONSTANT OF THE EXCHANGE FUNCTION
C       X          SOLUTION CONCENTRATION
C       T          TIME
C       FOX        EXCHANGER CONCENTRATION
C
C    INPUT
C       D, V, RO, Q, ALF, CO
C       HZ, HT, MT, N, IT, IZ
C       SLOPE, AINCP
C
C    OUTPUT
C       D, V, RO, Q, ALF, CO
C       HZ, HT
C       SLOPE, AINCP
C       T, X(I)
C       FOX(I)
C
C    METHOD
C       THE EXPLICIT METHOD DESCRIBED IN THE TEXT WITH A LINEAR
C       EXCHANGE FUNCTION
C
C.....................................................................

C    MAIN PROGRAM
       DIMENSION X(100), Y(100), FOX(100)
C
C    INPUT BASIC DATA
```

```
C
      READ(5,100) D, V, RO, Q, ALF, CO
      READ(5,101) HZ, HT, MT, N, IT, IZ
      WRITE(6,200) D, V, RO, Q, ALF, CO
      WRITE(6,201) HZ, HT
      READ(5,102) SLOPE, AINCP
      WRITE(6,204) SLOPE, AINCP
      NP1 = N + 1
      NM1 = N - 1
      DZ2 = D/(HZ*HZ)
      VZ = V/(2.*HZ)
      RQAC = (RO*Q*SLOPE)/(ALF*CO)
      FT = (1. + RQAC)/HT
C
C     SET THE BOUNDARY AND THE INITIAL CONDITIONS
C
      X(1) = 1.0
      DO 1 I = 2, NP1
    1 X(I) = 0.0
      KN = 0
      T = 0.0
C
C     BEGIN THE COMPUTATION OF X(I)
C
      DO 20 IIT = 1, MT
      DO 30 I = 2, N
      Y(I) = ((DZ2 - VZ)*X(I + 1) - (2.*DZ2 - FT)*X(I) +
     &(DZ2 + VZ)*X(I - 1))/FT
   30 CONTINUE
      Y(NP1) = Y(NM1)
      DO 40 J = 2, NP1
   40 X(J) = Y(J)
      KN = KN + 1
      T = T + HT
      IF(KN.NE.IT) GO TO 20
C
C     OUTPUT OF X(I) AND FOX(I)
C
      WRITE(6,203) T, (X(I), I = 1, N, IZ)
      DO 50 I = 1, N
   50 FOX(I) = AINCP + X(I)*SLOPE
      WRITE(6,205) (FOX(I), I = 1, N, IZ)
      KN = 0
   20 CONTINUE
  100 FORMAT(6F10.4)
  101 FORMAT(2F10.4,4I5)
  102 FORMAT(2F10.5)
  200 FORMAT(1H1, 14X, 'DISPERSION COEFFICIENT', F15.6/15X,
     &'FLOW VELOCITY', F15.6/15X, 'BULK DENSITY', F15.6/
```

```
     &15X, 'EXCHANGE CAPACITY', F15.6/15X, 'PORE FRACTION',
     &F15.6/15X, 'TOTAL CONCENTRATION', F15.6)
201   FORMAT(//14X, 'DEPTH INTERVAL', F15.6, 10X, 'TIME
     &INTERVAL', F15.6)
203   FORMAT(1H , 14X, 'TIME IS', F10.2//(10F13.7))
204   FORMAT(1H1, 'SLOPE OF THE EXCHANGE FUNCTION IS', F10.6,
     &'     INTERCEPT IS', F10.6)
205   FORMAT(//(10F13.7))
      STOP
      END
```


*U.S. GOVERNMENT PRINTING OFFICE: 1973 514-156/329 1-3

SELECTED WATER RESOURCES ABSTRACTS
INPUT TRANSACTION FORM

1. Report No. | 2. | 3. Accession No. W

4. Title CATION TRANSPORT IN SOILS AND FACTORS AFFECTING SOIL CARBONATE SOLUBILITY,

5. Report Date

6.

8. Performing Organization Report No.

7. Author(s)
Jurinak, Jerome J., Lai, Sung-Ho and Hassett, John J.

9. Organization
Utah State University, Logan, Utah 84322

10. Project No. 13030 FDJ

11. Contract/Grant No. 13030 FDJ

13. Type of Report and Period Covered

12. Sponsoring Organization

15. Supplementary Notes

Environmental Protection Agency Report No. EPA-R2-73-235, May 1973

16. Abstract A predictive model of cation transport in soils undergoing miscible displacement was developed and tested. A mass balance equation was formulated to include a general nonlinear cation exchange function. The model was applied to the transport of cations through an exchanger using five types of exchange functions. The model was further tested by conducting soil column studies which involved both homovalent and heterovalent exchange. Good agreement between experimental and predicted data was obtained.

Laboratory studies were also conducted to assess the affect of Mg^{+2} ion on the solubility of calcareous materials. Solubility was found to vary with the surface area and mineralogy of the carbonate material, and the degree of saturation of the water with respect to a given carbonate mineral. In waters unsaturated with respect to calcite, Mg^{+2} generally increased the solubility of calcite. The presence of Mg^{+2} decreased the solubility of dolomite in waters which were near saturation with respect to dolomite.
(Jurinak - Utah State)

17a. Descriptors ion transport*, calcium carbonate *, soil leaching, cation exchange, irrigation return flow, precipitation chemical, hardness (water).

17b. Identifiers solute transport*, carbonate solubility*, miscible displacement, carbonate saturometer.

17c. COWRR Field & Group 05B

18. Availability	19. Security Class. (Report)	21. No. of Pages	Send To:
	20. Security Class. (Page)	22. Price	WATER RESOURCES SCIENTIFIC INFORMATION CENTER U.S. DEPARTMENT OF THE INTERIOR WASHINGTON, D. C. 20240

Abstractor Jerome J. Jurinak | Institution Utah State University, Logan, Utah 84322